rijksuniversiteit groningen

Surface plasmons and effects of losses in propagating modes in a chain of silver nanoparticles

Author:
Xabier Inchausti Ezeiza

Supervisor:
Prof. dr. Jasper Knoester

Second supervisor:
Prof. dr. ir. Caspar van der Wal

Home university supervisor:
Dr. Jon Urrestilla Urizabal

June 26, 2015

Abstract

In this work a chain of 4000 silver nanoparticles embedded in a glass medium is considered, and its leftmost particle is excited by an electric field pulse of Gaussian shape. Considering Drude's model, losses of the system are taken into account by γ factor, which stands for the Ohmic losses, and different quantities, such as frequencies of excited modes and group velocities are calculated. Besides, these results are compared to those obtained from the dispersion relation of an infinite chain. The increase of losses affects the lifetime and propagation length of the plasmon; besides, although the response dispersion relation for an infinite chain seems to remain invariable, this is not the case for a finite chain. The mismatches are bigger for higher losses. Furthermore, plasmon propagation velocities are analysed, and an explanation for the mismatch of longitudinal modes close to the intersection point with the dispersion of light is suggested. Finally, some concepts to treat this problem from the energy transport point of view are introduced.

Contents

List of Figures

Chapter 1

Introduction

The interaction of electromagnetic radiation with an interface yields very interesting excitations in the surface. More precisely, a light wave exerts an external force in a dielectric/conductor interface, and this can lead to a collective oscillation of free electrons in the metal, in resonance with the incident light: this interaction between the surface charge and electromagnetic field of light create the so called *surface plasmon polaritons* (SPPs) [1]. Surface plasmon polaritons are propagating electromagnetic waves trapped at the surface of the conductor, and they are believed to have great potential in fields such as optics, magneto-optics and biosensing. In particular, they help us concentrate light in miniaturized structures whose length scales are smaller than the wavelength of light, which has given rise to a new research field in physics called plasmonics [1,2].

An example of these subwavelength structures can be a linear chain of metal nanoparticles placed very close to each other. Embedding this chain into a dielectric material gives the desired dielectric/conductor interface in which surface plasmon polaritons can be excited. By analysing the response of the nanoparticles to an excitation caused by an electromagnetic field we can derive interesting wave-guiding properties of this structure. In this work, we will simulate an electromagnetic Gaussian pulse which excites only the leftmost metallic sphere of a chain consisted of silver spherical nanoparticles. Assuming Drude's model for dielectric relative permittivity the damping factor γ is introduced, which quantifies the losses that happen in the system. Although it does not take all losses into account, its variation already affects the response of the chain. The effect and influences of the losses will be subject of interest in the propagation of plasmonic modes along the chain. Its response will be compared to the wave-guiding properties obtained from the dispersion relation of an infinite chain, and the variation produced by losses in the previously mentioned dispersion relation will also be considered. Two quantities of interest will be the imaginary part of the excited modes and the propagation velocities of them. Finally, some concepts will be introduced in order to make an analysis of this problem from the energy transport point of view, as plasmonic modes carry electromagnetic energy with themselves.

In chapter 2 some theory is developed in order to provide the reader the necessary background to understand the mechanism of our system, including the models that have been taken into account. All equations are given in SI units. Chapter 3 will show the parameters and methods used in order to perform the simulations. The results of them will be given in chapter 4, along with the comparison of the response obtained from the dispersion relation. A section will be introduced about energy transport considerations. Finally, conclusions and interesting features will be summarized in chapter 5, along with some suggestions for future research. Last two chapters contain acknowledgements and the bibliography used throughout this project.

Chapter 2

Theoretical foundations

2.1 Surface plasmon polaritons (SPPs)

Surface plasmon polaritons are collective oscillations of free electrons of the conductor that arise from the interaction between an electromagnetic field and the electron plasma of the conductor at a dielectric/conductor interface. In this kind of interface a surface mode is allowed whose electromagnetic field decays into both media; nevertheless, the wave can propagate along the surface: this mode is the surface plasmon. The momentum of the propagating surface plasmon is bigger than the momentum of the incident light: as the coupled light and plasmon have the same frequency, light momentum must be enhanced in order to generate propagating modes. There are several techniques by which this mismatch can be solved, such as prism coupling or the use of corrugated metal surfaces; more information about these methods can be found in references [1],[3] and [4]. Besides, localized plasmons can be excited at confined regions, such as a small, conducting single nanoparticle. The curved surface of the nanoparticle applies an effective restoring force to the free electrons of the conductor, which leads to a resonance. This resonance is the so called *localized surface plasmon*, since the plasmon is excited and remains in the particle [3]. The biggest advantage of this mode is that the plasmon can be excited by direct illumination due to the previously mentioned curved surface of the nanoparticle. Therefore, there is no need to enhance the momentum of the incident light, which is the case for propagating surface plasmons, making localized modes much easier to obtain.

2.2 Spherical conducting nanoparticle in an electric field

2.2.1 Quasi-static approximation

As it has been stated in the abstract of this report, the system of interest is a linear chain of silver nanospheres embedded in glass. The first particle is excited by an electric pulse. First, it is wise to look at the response of a single nanoparticle under an electric field. For this purpose we will first consider the quasi-static approximation developed in reference [3]. This is a simplified problem of a particle in an electrostatic field: we assume that the particle is much smaller than the wavelength λ of light in the surrounding medium, and that the phase of the electric field is constant over the volume. Considering this model, we are able to obtain the expression for the induced dipole moment in the particle:

$$\vec{p} = 4\pi\epsilon_0\epsilon_m a^3 \frac{\epsilon - \epsilon_m}{\epsilon + 2\epsilon_m}\vec{E} \tag{2.1}$$

where we can see that the dipole moment is proportional to the magnitude of the applied field. Besides, the assumption of an electrostatic field implies that the nanoparticles can be replaced by a point dipole located at the center of the sphere. If we introduce the definition for polarizability $\vec{p} = \alpha^{(0)}\vec{E}$, this last parameter is defined in the following way:

$$\alpha^{(0)} = 4\pi\epsilon_0\epsilon_m a^3 \frac{\epsilon - \epsilon_m}{\epsilon + 2\epsilon_m} \tag{2.2}$$

Note that in this expression ϵ_m is the relative permittivity of the medium which surrounds our sphere, ω is the frequency of the oscillating field and that $\epsilon(\omega)$ is the complex dielectric constant of the particle, which will be stated in the following subsection. Looking at the polarizability, it is clear that it is resonantly enhanced when the magnitude of the denominator reaches a minimum. For the case of a slowly-varying $\mathrm{Im}[\epsilon(\omega)]$, this is obtained when

$$Re[\epsilon(\omega)] = -2\epsilon_m \tag{2.3}$$

This relationship is called the *Fröhlich condition*, and the mode that fulfills this condition in the oscillating field is called the *dipole surface plasmon* of the nanoparticle [4].

Up to this point we can remark two important features. In the first place, we can see from the Fröhlich condition that the real part of the dielectric constant must be negative. This is the case for many metals, whose conduction electrons can be assumed to be reasonably free, at frequencies smaller than plasma frequency [5]. On the other hand, although the frequency of the applied field clearly plays a role in this system, we have only considered the electrostatic case. If we consider that the incident field is a plane-wave of the form $\vec{E}(t) = \vec{E}_0 e^{-i\omega t}$, the induced dipole moment is also multiplied by the same time-dependent factor, which yields the oscillating dipole moment $\vec{p}(t) = \alpha^{(0)}\vec{E}_0 e^{-i\omega t}$ with the same frequency as the external field.

So far we have derived some important magnitudes in order to understand the physics involved in our single-particle system. In order to do so the quasi-static approach has been considered, which is very useful to understand the problem due to its simplicity. Unfortunately, it is not very accurate regarding our system, since we are not dealing with electrostatic fields. This means that we also have to include the radiation damping, as the oscillation amplitude is not constant throughout time. Besides, the polarizabily should also be corrected for spatial dispersion [6]. Therefore, the polarizability of the nanoparticles can be expanded up to the m^{th} order of the wavenumber k of the driving field [7]. Including the corrections up to third order, we get the following expression, as stated in reference [6], where $\alpha^{(0)}$ is the bare polarizability derived from the quasi-static approximation.

$$\frac{1}{\alpha} = \frac{1}{\alpha^{(0)}} - \frac{k^2}{4\pi\epsilon_0\epsilon_m a} - \frac{ik^3}{6\pi\epsilon_0\epsilon_m} \tag{2.4}$$

2.2.2 Drude model

The optical properties of a metal can be very well described by a complex dielectric function that depends on the frequency of the incident light, as we have previously noted briefly. The dielectric function is determined mainly by the motion of the conduction electrons that can move freely within the metal. The presence of an external electric field displaces the electrons of our metal nanoparticle: using Drude-Sommerfeld model and solving the equation of motion of free-electron gas we will get an expression for the permittivity of the nanosphere, as described in reference [8].

As stated before, the applied electric field $\vec{E}(t) = \vec{E}_0 e^{-i\omega t}$ causes a displacement of all electrons, giving the dipole moment $\vec{p} = -e\vec{r}$, which also creates a polarization vector in the particle, $\vec{P} = n\vec{p}$, where e is the absolute value of the charge of the electron and n is the free-electron density. Using Drude's model, which takes into account the collision of electrons and therefore includes a damping frequency γ, the equation of motion is given by

$$m_e \frac{d^2\vec{r}}{\mathrm{d}t^2} + m_e\gamma\frac{d\vec{r}}{\mathrm{d}t} = -e\vec{E}_0 e^{-i\omega t} \tag{2.5}$$

which is a driven damped harmonic equation. Here m_e is the effective mass of the electrons and $\vec{r}$ the displacement vector. By substituting $\vec{r}(t) = \vec{r}_0 e^{-i\omega t}$ in the equation, we get the solution:

$$\vec{r}(t) = \frac{e\vec{E}}{m_e(\omega^2 + i\gamma\omega)} e^{-i\omega t} \tag{2.6}$$

Finally, as

$$\vec{P} = n\vec{p} = -e\vec{r} \tag{2.7}$$

$$\vec{P} = \epsilon_0 \chi_e(\omega)\vec{E} \tag{2.8}$$

$$\epsilon(\omega) = 1 + \chi_e(\omega) \tag{2.9}$$

the full expression of the complex dielectric function is given by

$$\epsilon(\omega) = 1 - \frac{\omega_p^2}{\omega^2 + i\gamma\omega} \tag{2.10}$$

where ω_p is the plasma frequency ($\omega_p = \sqrt{ne^2/m_e\epsilon_0}$). The previous equation is known as the Drude model. In our simulations a more general Drude model fit to experimental data is used, in which each newly introduced parameter depend on the material of the nanoparticle (extracted from [9] and [10]):

$$\epsilon(\omega) = \eta - \frac{\beta\omega_p^2}{\omega^2 + i\gamma\omega} \tag{2.11}$$

2.2.3 Electromagnetic fields of a points source

In the previous sections we have dealt with a metal nanoparticle being excited by a plane-wave electric field, which is the cause of the motion of the free electrons. Since the field is oscillating, so are the charges; consequently, the induced oscillating dipole moment oscillates with the same frequency as the external field. The nanoparticles can be replaced by point dipoles placed in the center of the particle. As oscillating charges create an electric field in the space, so will the oscillating dipoles, which is expressed by the next equation [13]:

$$\vec{E}_{dip}\left(\vec{p},\vec{r},\omega\right) = \frac{1}{4\pi\epsilon_0\epsilon_m}\left[(1 - \frac{i\omega r}{v})\frac{3(\hat{r}\cdot\vec{p})\hat{r} - \vec{p}}{r^3} + \left(\frac{\omega}{v}\right)^2 \frac{\vec{p} - (\hat{r}\cdot\vec{p})}{r}\right] e^{i\frac{\omega}{v}r - i\omega t} \tag{2.12}$$

where $\vec{r}$ is the vector going from the dipole to any point in the space, $\vec{p}$ is the dipole moment, ω is the frequency of the oscillating dipole and v the velocity of light in the medium. It is clear that in both the external electric field and the oscillating dipole the time-dependent component is given by the exponential $e^{i\frac{\omega}{v}r - i\omega t}$. Due to this, in this subsection we will describe another method to express the spatial-dependent electromagnetic fields created by a point source, bearing in mind that time-dependence is given by the previous exponential.

In electromagnetic theory, the *Green's function* is a very important concept in order to define electromagnetic fields originated from a point source, which in our case is the point dipole. We will first begin by defining the electric field in terms the *dyadic Green's function* $\mathbf{G}$ [8]:

$$\vec{E}(\vec{r}) = \omega^2\mu_0\mu_m\mathbf{G}(\vec{r},\vec{r_0})\vec{p} \tag{2.13}$$

where ω is the frequency of the oscillating dipole, μ_0 and μ_m are the magnetic permeability in vacuum and the relative permeability respectively; $\vec{r}$ is the coordinate where the field is created, while $\vec{r_0}$ gives the position of the dipole, and $\vec{p}$ is the dipole moment. The Green's function is derived in full detail in reference [8]; we will only state the result here:

$$\mathbf{G}(\vec{r},\vec{r_0}) = \left[\mathbf{I} + \frac{1}{k^2}\vec{\nabla}\vec{\nabla}\right] G_0(\vec{r},\vec{r_0}) \tag{2.14}$$

where $k = \frac{\omega}{v}$ is the wavevector of the field and G_0 is the *scalar* Green's function, given by:

$$G_0(\vec{r},\vec{r_0}) = \frac{e^{ik|\vec{r}-\vec{r_0}|}}{4\pi|\vec{r}-\vec{r_0}|} \tag{2.15}$$

If we perform the calculus of equation 2.14, the result gives the following definition for dyadic Green's function in Cartesian coordinates [8]:

$$\mathbf{G}(\vec{r},\vec{r_0}) = \frac{e^{ikR}}{4\pi R}\left[\left(1+\frac{ikR-1}{k^2R^2}\right)\mathbf{I}+\frac{3-3ikR-k^2R^2}{k^2R^2}\frac{\vec{R}\vec{R}^T}{R^2}\right] \tag{2.16}$$

In this new expression $\vec{R} = \vec{r} - \vec{r_0}$ is the relative position vector and R = $|\vec{R}|$ its magnitude.

Furthermore, the magnetic field $\vec{H}$ can also be written in terms of $\mathbf{G}$. We start by writing the Faraday equation for time-harmonic fields [8]:

$$\vec{\nabla}\times\vec{E}(\vec{r}) = -\mu_0\mu_m\frac{\delta\vec{H}}{\delta t} = i\omega\mu_0\mu_m\vec{H}(\vec{r}) \tag{2.17}$$

Introducing equation 2.13 in 2.17 and isolating $\vec{H}(\vec{r})$ we get the following expression for the magnetic field created by a point dipole [8]:

$$\vec{H}(\vec{r}) = i\omega[\vec{\nabla}\times\mathbf{G}(\vec{r},\vec{r_0})]\vec{p} \tag{2.18}$$

2.3 Chain of metal nanoparticles

2.3.1 Coupling of dipoles

Now that the physics of a single metal nanoparticle excited by an external electric field have been shown in detail, we will proceed by analysing a linear chain of metal nanospheres. The chain is oriented along the direction $\hat{x}$, and it is embedded in a medium whose relative permittivity is ϵ_m. All the particles are identical, and the center-to-center distance among them is also the same, defined by parameter d, as it can be seen in figure 3.1.

If any particle, denoted with index n, is excited by an external electric field, an oscillating electric dipole moment is generated. This, according to equation 2.13, will induce an electric field in the surroundings, resulting in the generation of induced electric dipole moments in the other particles. The newly excited particles will subsequently produce electric fields around them, affecting the other spheres. Note that the dipole moments of the spheres can be approximated as point dipole moments under the conditions $a \ll \lambda$ and $d \geq 3a$, where a is the radius of the sphere [12]. Finally, we will get a coupled system in which each particle influences the rest, and we will ultimately turn our array of nanoparticles into a chain of oscillating dipole moments. According to expression $\vec{p} = \epsilon_0\epsilon_m\alpha\vec{E}$, the induced dipole moment in the n^{th} particle is given by:

$$\vec{p}_n = \alpha\left[\vec{E}_{ext}(\vec{r}_n) + \sum_{m\neq n}\vec{E}_{dip}(\vec{r}_n,\vec{r}_m)\right] \tag{2.19}$$

where $\vec{E}_{ext}(\vec{r}_n)$ is the applied external field in particle n and $\vec{E}_{dip}(\vec{r}_n,\vec{r}_m)$ is the electric field induced by the dipole of m^{th} sphere in the n^{th} particle. According to the previous subsection, the electric field generated by an electric dipole moment is given by equation 2.13; substituting this in equation 2.19 we get the following result:

$$\vec{p}_n = \alpha\left[\vec{E}_{ext}(\vec{r}_n) + \sum_{m\neq n}\omega^2\mu_0\mu_m\mathbf{G}(\vec{r}_n,\vec{r}_m)\vec{p}_m\right] \tag{2.20}$$

We can write this equation for all N particles in the chain; by doing so, we will obtain a linear system described below:

$$\begin{pmatrix} -\vec{E}_{ext}(\vec{r}_1) \\ -\vec{E}_{ext}(\vec{r}_2) \\ \vdots \\ -\vec{E}_{ext}(\vec{r}_n) \end{pmatrix} = \begin{pmatrix} -\mathbf{I}\frac{1}{\alpha} & \omega^2\mu_0\mu_m\mathbf{G}(\vec{r}_1,\vec{r}_2) & \cdots & \omega^2\mu_0\mu_m\mathbf{G}(\vec{r}_1,\vec{r}_N) \\ \omega^2\mu_0\mu_m\mathbf{G}(\vec{r}_2,\vec{r}_1) & -\mathbf{I}\frac{1}{\alpha} & \cdots & \omega^2\mu_0\mu_m\mathbf{G}(\vec{r}_2,\vec{r}_N) \\ \vdots & \vdots & \ddots & \vdots \\ \omega^2\mu_0\mu_m\mathbf{G}(\vec{r}_N,\vec{r}_1) & \omega^2\mu_0\mu_m\mathbf{G}(\vec{r}_N,\vec{r}_2) & \cdots & -\mathbf{I}\frac{1}{\alpha} \end{pmatrix} \begin{pmatrix} \vec{p}_1 \\ \vec{p}_2 \\ \vdots \\ \vec{p}_n \end{pmatrix} \tag{2.21}$$

This is a simple matrix relation relating the external field applied on the chain and the induced dipole moments, where the coupling matrix contains dyadic Green's functions within it. Note that the matrix is symmetric, since $\mathbf{G}(\vec{r}_n,\vec{r}_m) = \mathbf{G}(\vec{r}_m,\vec{r}_n)$, as the distance between the points given by vectors $\vec{r}_n, \vec{r}_m$ is the quantity of interest in Green's functions.

2.3.2 Polarizations

In the previous section we derived the coupling matrix of the chain's electric field and electric dipolar moments, where a three-dimensional Green's tensor is included in the off-diagonal elements of the matrix. At the beginning of the previous section we have stated that all nanoparticles are identical, placed along a line and with the same center-to-center distance: this implies some symmetries in the chain, so the coupling matrix can be simplified.

In this subsection we will turn Green's tensors in scalars by taking polarizations into account. There are two different main directions for the electric field: the longitudinal and the transversal direction. The longitudinal polarization of the field is parallel to the linear chain, while the transversal polarization is orthogonal to it, so that both polarizations can be decoupled. Consider equation 2.16 in which Green's tensor is given in terms of Cartesian coordinates, and assume that the chain axis is the $\hat{x}$-direction. These results in $(\vec{r} \parallel \vec{p}_n)$ for longitudinal polarization, and $(\vec{r} \perp \vec{p}_n)$ in the transversal case. As a result, the term corresponding to longitudinal polarization is:

$$\mathbf{G}_l = 2\left(-\frac{iv}{\omega R^2} + \frac{v^2}{\omega^2 R^3}\right) e^{i\frac{\omega}{v}R} \tag{2.22}$$

while the other two diagonal elements are the transversal component of Green's tensor:

$$\mathbf{G}_t = \left(\frac{1}{R} + \frac{iv}{\omega R^2} - \frac{v^2}{\omega^2 R^3}\right) e^{i\frac{\omega}{v}R} \tag{2.23}$$

Therefore, we can decouple the resulting electric and dipole moments in longitudinal and transversal polarizations, which might be of interest in order to perform faster calculations. Besides, one difference that can be seen between both expressions is that there is a term $1/R$ missing in the longitudinal relation. This means that the contribution from longitudinal polarization does not play a role in the far field interactions [11], so that we can expect that the longitudinal term of the dipoles will decay faster in the chain.

2.4 Dispersion relation and damping

2.4.1 Derivation of dispersion relation

In this project we are interested in the chain's response to an external electric field and the excited surface plasmon waves, in order to look at the wave-guiding properties of our linear structure. For that purpose we have performed simulations of the system; nevertheless, there is another tool which encloses the properties we would like to find out more about: the dispersion relation. The dispersion relation describes the properties of a wave travelling through a medium by relating wavenumbers q and angular frequency ω of the wave. From here other quantities such as phase velocity or group velocity can be derived. These calculations are done for an infinite chain.

We start by calculating the normal modes of the chain: for this purpose the external electric field ($\vec{E}_{ext}(\vec{r}_n) = 0$, for all n) is switched off. Equation 2.12 (ref. [11]) is substituted in equation 2.19, and the resulting expression can be simplified further by considering that the distance

between nearest-neighbour nanoparticles is the same.Including the corrected form of the polarizability as a function of frequency, which already includes corrections for spatial dispersion and radiation damping (equation 2.4), we get the following result [12]:

$$\vec{p}_n = \frac{\alpha(\omega)}{4\pi\epsilon_0\epsilon_m}\left\{\sum_{m\neq n}\left[(1-i\frac{\omega}{v}|n-m|d)\frac{3(\hat{r}\cdot\vec{p}_m)\hat{r}-\vec{p}_m}{|n-m|^3d^3}+\right.\right.$$

$$\left.\left.+\left(\frac{\omega}{v}\right)^2\frac{\vec{p}_m-(\hat{r}\cdot\vec{p}_m)\hat{r}}{|n-m|d}\right]e^{i\frac{\omega}{v}|n-m|d}\right\} \tag{2.24}$$

Now, considering an $infinite$ chain, the normal modes can be expressed in the form of Bloch waves with wavenumber q, such as $\vec{p}_n \propto e^{iqnd}$. Besides, longitudinal and transversal polarizations can be separated, making calculations easier.

For the longitudinal polarization, $(\vec{r} \parallel \vec{p}_n)$, scalar multiplications $\vec{r}\cdot\vec{p}_n$ give a multiplication between their magnitudes. Substituting the Block waves for the dipole moments and defining index $j = |n-m|$, we get this identity:

$$0 = 1 + \frac{\alpha(\omega)}{2\pi\epsilon_0\epsilon_m d^3}\sum_{m\neq n}^{\infty}\left(\frac{1}{j^3}-\frac{i\omega d}{vj^2}\right)\left(e^{i(\frac{\omega}{v}+q)d}+e^{i(\frac{\omega}{v}-q)d}\right) \tag{2.25}$$

We now define the polylogarithm function $Li_s(z)$, taken from [14]

$$Li_s(z) \equiv \sum_{k=1}^{\infty}\frac{z^k}{k^s} \tag{2.26}$$

We finally get the dispersion relation for the infinite chain in longitudinal polarization [13]:

$$0 = 1 - \frac{\alpha(\omega)}{2\pi\epsilon_0\epsilon_m d^3}\left\{Li_3\left(e^{i(\frac{\omega}{v}+q)d}\right)+Li_3\left(e^{i(\frac{\omega}{v}-q)d}\right)-\right.$$

$$\left.-\frac{i\omega d}{v}\left[Li_2\left(e^{i(\frac{\omega}{v}+q)d}\right)+Li_2\left(e^{i(\frac{\omega}{v}-q)d}\right)\right]\right\} \tag{2.27}$$

Similarly, we derive the dispersion for transversal polarization by taking $(\vec{r}\perp\vec{p}_n)$ condition, so that $(\vec{r}\cdot\vec{p}_n)=0$. Introducing Bloch waves for dipoles and the substitutions to get the polylogarithm function, we get a different equation for the dispersion relation of the transversal polarization.

$$0 = 1 + \frac{\alpha(\omega)}{4\pi\epsilon_0\epsilon_m d^3}\left\{Li_3\left(e^{i(\frac{\omega}{v}+q)d}\right)+Li_3\left(e^{i(\frac{\omega}{v}-q)d}\right)-\right.$$

$$-\frac{i\omega d}{v}\left[Li_2\left(e^{i(\frac{\omega}{v}+q)d}\right)+Li_2\left(e^{i(\frac{\omega}{v}-q)d}\right)\right])-$$

$$\left.-\frac{\omega^2d^2}{v^2}\left[Li_1\left(e^{i(\frac{\omega}{v}+q)d}\right)+Li_1\left(e^{i(\frac{\omega}{v}-q)d}\right)\right]\right\} \tag{2.28}$$

The difference between equations 2.27 and 2.28 comes from the absence of 1$^{\text{st}}$ order polylogarithm functions $Li_1(z)$ in the longitudinal dispersion relation. This comes from the missing $1/R$ term as seen in equation 2.22, indicating that longitudinal modes have no far field interactions, consequently differing from the transversal dispersion relation.

Solving this equations for real q we get their corresponding angular frequencies, $\omega(q)$, which are complex numbers. The imaginary part of $\omega = \omega_r + i\omega_i$ is related to the decay of the mode in time, as we will show in a later section; as a result the harmonic wave $e^{-i(\omega_r+i\omega_i)t} = e^{-i\omega_r t+\omega_i t}$ decays only if $\omega_i < 0$. On the other hand, the each member of the series converges only if $\omega_i > 0$. A convergence problem arises from the mathematical shape of the equation, but we know that physically the condition $\omega_i < 0$ must be satisfied. In order to sort out the mathematics, there is a tool we can use to solve the problem: the analytical continuation.

2.4.1.1 Analytical continuation

Analytical continuation is a technique to extend the domain of a function, so we can evaluate the function at a point which is not included in the domain. The mathematical expression that we want to analytically continue is the polylogarithm function, which converges if $\omega_i > 0$, while we are interested in $\omega_i < 0$. In order to evaluate the function at negative imaginary angular frequencies, we will use the following mathematical identity [15]:

$$Li_s(z) + (-1)^s Li_s(1/z) = \frac{(2\pi i)^s}{\Gamma(s)} \zeta\left(1-s, \frac{1}{2} + \frac{\ln(-z)}{2\pi i}\right) \tag{2.29}$$

where $z = e^{i(\frac{\omega}{v} \pm q)d}$, $|z| < 1$ for convergence and function ζ is the Hurwitz zeta function [14]. Therefore, if $|z| > 1$, we can calculate $Li_s(z)$ from the previous relation, as $Li_s(1/z)$ is convergent. The Hurwitz zeta function is defined in the following way:

$$\zeta(s', C) = \frac{\Gamma(1-s')}{2\pi i} \oint \frac{z^{s'-1} e^{Cz}}{1-e^{Cz}} dz \tag{2.30}$$

for Re(s') ≤ 1, which it is fulfilled since $s' = 1$–s and we are considering only $s = 1, 2, 3$; which are the orders of the polylogarithm function. The contour integral is evaluated using Cauchy's residue theorem [16]. We will start by expanding the exponentials in the integral to obtain the the value of the pole and its order, i.e. the point where the denominator of the function becomes 0, and its exponent.

$$\begin{aligned} I(z, s') &= \oint \frac{z^{s'-1} e^{Cz}}{1-e^{Cz}} dz = \oint \frac{z^{s'-1}(1 + Cz + \frac{1}{2}(Cz)^2 + \frac{1}{6}(Cz)^3 + ...)}{1 - 1 - z - \frac{1}{2}z^2 - \frac{1}{6}z^3 + ...} dz = \\ &= \oint \frac{z^{s'-2}(1 + Cz + \frac{1}{2}(Cz)^2 + \frac{1}{6}(Cz)^3 + ...)}{-1 - \frac{1}{2}z - \frac{1}{6}z^2 + ...} dz = \\ &= \oint \frac{(1 + Cz + \frac{1}{2}(Cz)^2 + \frac{1}{6}(Cz)^3 + ...)}{-z^{2-s'}(1 + \frac{1}{2}z + \frac{1}{6}z^2 + ...)} dz \end{aligned} \tag{2.31}$$

So we have a pole at $z = 0$ of order $2 - s'$. In general, considering a single pole of order n, Cauchy's residue theorem states:

$$I(z, n) = \oint \frac{f(z)}{z^n} dz = 2\pi i \operatorname{Res}_{z=z_0} f(z) \tag{2.32}$$

The residue is calculated in the following way [16]:

$$\operatorname{Res}_{z=z_0} f(z) = \lim_{z \to z_0} \frac{1}{(n-1)!} \frac{d^{n-1}}{dz^{n-1}} f(z) z^n \tag{2.33}$$

where n is the order of the pole. In our case,

$$f(z) = -\frac{1 + Cz + \frac{1}{2}(Cz)^2 + \frac{1}{6}(Cz)^3 + ...}{1 + \frac{1}{2}z + \frac{1}{6}z^2 + ...} \tag{2.34}$$

and

$$n = 2 - s' = \begin{cases} 2 & \text{if } s = 1, s' = 1 - s = 0 \\ 3 & \text{if } s = 2, s' = 1 - s = -1 \\ 4 & \text{if } s = 3, s' = 1 - s = -2 \end{cases} \tag{2.35}$$

The residue involves derivatives of function $f(z)$ up to third order. This is a long calculation, so we will just state the results:

$$\operatorname{Res}_{z=0} \begin{cases} \frac{1}{2}(1 - 2C) & \text{if } n = 2, s = 1 \\ \frac{1}{12}(-1 + 6C - 6C^2) & \text{if } n = 3, s = 2 \\ \frac{1}{12}(-C + 3C^2 - 2C^3) & \text{if } n = 3, s = 2 \end{cases} \tag{2.36}$$

Using 2.35 and 2.36 and substituting them in 2.32 we can compute the Hurwitz zeta function, which gives:

$$\zeta(1-s,C) = \frac{\Gamma(s)}{2\pi i}\oint \frac{z^{-s}e^{Cz}}{1-e^{Cz}}dz = \begin{cases} \frac{1}{4\pi i}(1-2C) & \text{if } s=1, \\ \frac{1}{24\pi i}(-1+6C-6C^2) & \text{if } s=2 \\ \frac{1}{12\pi i}(-C+3C^2-2C^3) & \text{if } s=3 \end{cases} \tag{2.37}$$

And finally, the analytical continuation for orders of polylogarithm $s = 1, 2, 3$ are the following:

$$Li_1(z) - Li_1(1/z) = \frac{1}{2}(1-2C) \tag{2.38}$$

$$Li_2(z) + Li_2(1/z) = \frac{\pi}{12}(-1+6C-6C^2) \tag{2.39}$$

$$Li_3(z) - Li_3(1/z) = \frac{-\pi^2 i}{16}(-C+3C^2-2C^3) \tag{2.40}$$

where $C = \frac{1}{2} + \frac{\ln(-z)}{2\pi i}$. Equations 2.38-2.40 enable us to fix the divergence problem of the dispersion relation raising from ω_i ¡ 0, so we can fully solve our physical system. By plotting both dispersion relations, we see that $\omega(q)$ is a continuous line for longitudinal polarization, while the dispersion relation consists of two anti-crossing lines which meet the light dispersion line at one of their ends. This splitting is caused by the retardation effects of the system ([13]). The dispersion relations for longitudinal and transversal modes are presented below, using the parameters given in [9], [10]. Graphs are shown in 2.1.

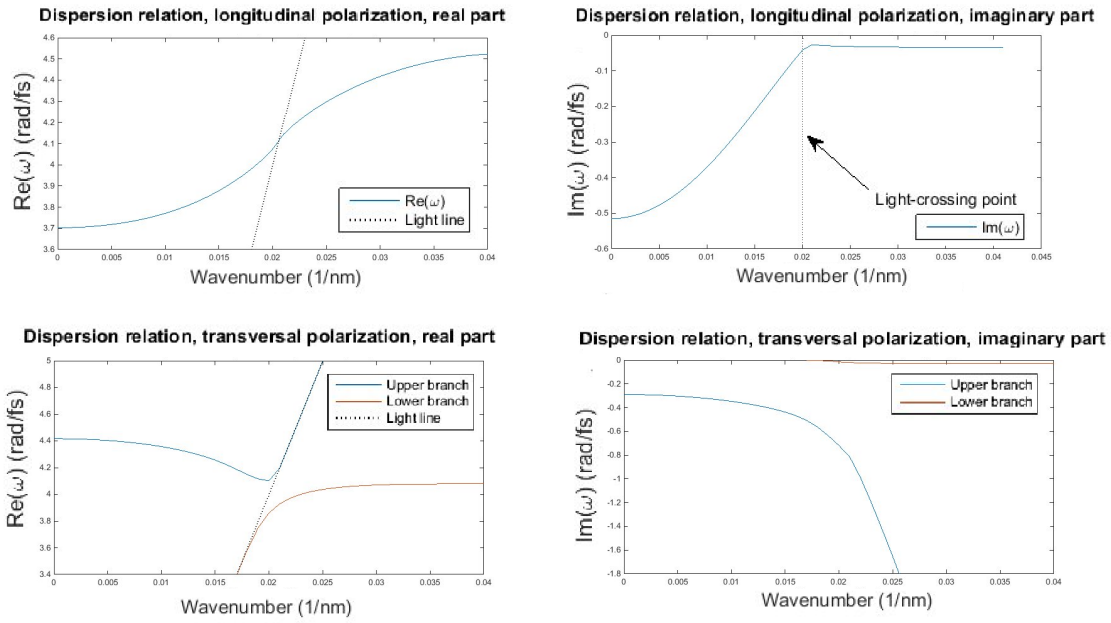

Figure 2.1: Dispersion relations for longitudinal and transversal polarizations, real and imaginary parts, for an infinite chain.

2.4.2 Group velocity

The dispersion relation is a very useful relation that enables us to get some very interesting wave-guiding properties of our system, for example, the *group velocity* [17]. The group velocity is the propagation velocity of the wave that, in our case, consist of the different alignments of the oscillating dipoles. It is defined as the slope of the dispersion relation:

$$v_g = \frac{\partial \omega(q)}{\partial q} \tag{2.41}$$

In order to get this physical quantity, we will derive the dispersion relations for the longitudinal and transversal modes. Since the dispersion relation is a function of ω and q, and $\omega = \omega(q)$, we can use the chain rule in the derivation to get the group velocity. If we take the dispersion relation function $F(q, \omega(q)) = 0$, the group velocity is

$$v_g = \frac{\partial \omega(q)}{\partial q} = -\frac{\frac{\partial F}{\partial q}}{\frac{\partial F}{\partial \omega}} \tag{2.42}$$

For example, substituting $z^+ = e^{i(\frac{\omega}{v}+q)d}$ and $z^- = e^{i(\frac{\omega}{v}-q)d}$, this is the equation of the group velocity for longitudinal modes:

$$v_g, l = \frac{-i\alpha d \left\{ Li_2(z^+) - Li_2(z^-) - \frac{i\omega d}{v} \left[Li_1(z^+) + Li_1(z^-) \right] \right\}}{\frac{\partial \alpha}{\partial \omega} \left\{ Li_3(z^+) + Li_3(z^-) - \frac{i\omega d}{v} \left[Li_2(z^+) + Li_2(z^-) \right] \right\} - \frac{\alpha \omega}{dv^2} \left[Li_1(z^+) + Li_1(z^-) \right]} \tag{2.43}$$

The same can be done for the transversal polarization, but due to its length we will omit this derivation here.

2.4.3 Propagation length

The propagation length is a measure of how far can a mode can travel before it decays completely and the signal is lost. It is defined by the fraction between the group velocity and the imaginary part of the angular frequency of the mode. This means that if we increase the losses, which are related to the imaginary part of the frequency, we will get shorter propagations. Its definition is as follows:

$$\ell = \frac{v_g}{\omega_i} \tag{2.44}$$

2.4.4 Damping of the waves in the chain

We have stated earlier that the imaginary part of the angular frequency ω of the mode of the chain is related to the decay of the wave or, in other words, to the damping of the system. Two types of damping can be identified in our model:

- *Radiative*: our waves (plasmons) become photons due to interactions with light, so radiation is emitted. These losses only happen for those modes which are above the light line in the dispersion relation, since for the same frequency the wavenumber of the chain modes is smaller than that of the light.
- *Ohmic*: damping which is related to the velocity of the electrons in the equation of motion, given by parameter γ in the Drude model. It can be viewed as a counterpart of the damping in harmonic oscillators, which are also linked to the velocity component. It describes how the amplitude of the signal decreases in time.

The imaginary part of the mode frequencies gives the lifetime of the modes, since the lifetime is defined as $1/\omega_i$. Both radiative and Ohmic losses affect the lifetime of a mode; therefore, they also contribute to ω_i. As an example, we show how the Ohmic losses described by γ affect the polarizability of the particles.

From $\alpha^{(0)}$ (eq. 2.2), according to reference [18], we derive the following expression:

$$\alpha(\omega) = 4\pi\epsilon_0\epsilon_m a^3 \frac{\omega_{sp}^2}{\omega_{sp}^2 - \omega^2 - i\gamma\omega} \tag{2.45}$$

where $\omega_{sp} = \omega_p/\sqrt{(3)}$ is the surface plasmon frequency of electrons. Expanding around $\omega \approx \omega_{sp}$, which is the resonance frequency gives:

$$|\alpha(\omega)|^2 = 4\pi^2\epsilon_0^2\epsilon_m^2 a^6 \frac{\omega_{sp}^2}{(\omega_{sp}-\omega)^2+\gamma^2/4} \tag{2.46}$$

This is a Lorentzian with a full width at half maximum of γ, which is the Ohmic damping term. Therefore, larger damping terms result in a broader polarizability function.

2.5 Energy transport

Up to now we have seen that the oscillating dipole moments induced in each particle by the external field leads to the generation of electromagnetic fields by the dipole moments; besides, the pattern of the dipoles show us waves propagating in the chain. This oscillating trend goes along the chain passing through all particles, changing the amplitude of each oscillation as it goes by. Due to this, the electromagnetic field around each particle varies, and so happens to the electromagnetic energy of the fields. In order to observe this trend, how electromagnetic fields follow the wave and, consequently, how the electromagnetic energy behaves along the wave, we will calculate a new physical quantity: the energy transport velocity, v_E.

Firstly, it is convenient to introduce the *Poynting* vector, which represents the energy flux density of the electromagnetic field [8]:

$$\vec{S} = \vec{E} \times \vec{H} \tag{2.47}$$

Besides, it is interesting to calculate the time average value of the Poynting vector, as it describes the net power flux density taking into account the dissipation of energy in the system. Considering time-harmonic fields and linear media, the time average Poynting vector is

$$\left\langle \vec{S} \right\rangle = \frac{1}{2} Re[\vec{E} \times \vec{H}^*] \tag{2.48}$$

On the other hand, the electromagnetic energy density is calculated as follows:

$$W = \frac{1}{2}(\epsilon_0\epsilon_m|E|^2 + \mu_0\mu_m|H|^2) \tag{2.49}$$

where $E = |\vec{E}|$ and $H = |\vec{H}|$ are the magnitudes of the fields. In a non-dispersive medium, and assuming harmonic time-dependence, the time average energy density is [20]:

$$\langle W \rangle = \frac{1}{4}(\epsilon_0\epsilon_m|E|^2 + \mu_0\mu_m|H|^2) \tag{2.50}$$

Finally, the velocity of energy transport through the medium is defined as [19]:

$$v_E = \frac{\left\langle \vec{S} \right\rangle}{\langle W \rangle} \tag{2.51}$$

The value of the energy transport velocity is an interesting quantity to us, as it is the same as the group velocity of the wave only in a non-absorbing medium [19].

Chapter 3

Description of simulation

3.1 Chain parameters

Once that all the theoretical basis of this project has been clarified, we will now look at the physical features we have assumed during the simulations. Our system is a linear chain of identical metal nanoparticles embedded in a dielectric medium.

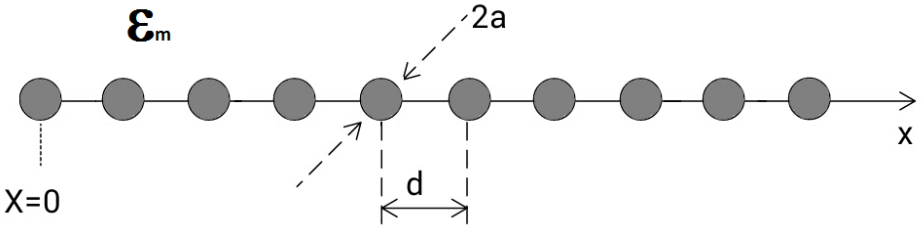

Figure 3.1: Chain of silver nanoparticles embedded in glass, with relative permittivity ϵ_m.

Our chain contains N = 4000 particles, so it gives us a good resolution in order to see the excited modes. We have chosen glass to be our medium through which light propagates and reaches the nanoparticles. As a result, the relative permittivity of the medium is $\epsilon_m = 2.25$ and the magnetic permeability is $\mu_m = 1$. Consequently, the index of refraction in the medium is $n = \sqrt{\epsilon_m \mu_m} = 1.5$. Regarding the spheres, we take silver as material and a radius of $a = 25$nm, while the center-to-center distance is $d = 75$nm between the nearest spheres, so that the conditions for point-dipole approximation are satisfied ($a \ll \lambda$ and $d \geq 3a$). In total, the chain's length is L = 299,975nm ≈ 0.3 μm. On the other hand, we will remember now the experimental fit to the Drude model for the relative permittivity of silver given in equation 2.11, and we will define the parameters of the silver nanospheres, according to references [9] and [10]:

$$\eta = 5.45 \ ; \ \beta = 0.73 \ ; \ \omega_p = 17.2 \text{ rad/fs} \ ; \ \gamma = 0.0835 \text{ PHz} \tag{3.1}$$

3.2 Excitation of chain: Gaussian pulse propagation

We have initially mentioned that only the leftmost particle of the chain would be excited by an external electrical field. In this section we will explain the method we have used to do so, and also to calculate the time-dependence of the induced dipole moments in the chain in order to be able to track the excited chain mode. We have chosen a Gaussian-shaped time-dependent electric field pulse to excite a single particle of the chain. This pulse represents a real excitation of a laser beam, which shines on the particle only for a short amount of time. These are the steps we will follow in order to get the response of the chain to our pulse:

1. The Gaussian pulse will have a suitable width in time domain in order to be able to track the chain modes nicely.

2. Calculations in the time domain are quite tricky; due to this, we will perform a Fourier transform to change the Gaussian from time domain to frequency domain and run our calculations there. The Gaussian pulse will be a Gaussian also in the frequency domain, but the excited dipole moments and the later generated electromagnetic fields will be harmonic waves in the frequency domain, so calculations will be easier to make.

3. We will solve equation 2.21 for different frequencies in the grid and for the two polarizations: longitudinal and transversal. We will assign a constant arbitrary value to the external electric field for the first particle, which will be its amplitude, and the rest will be null: this way we are only exciting the first particle. Solving the linear system in equation 2.21 we will get the induced dipole moment of each particle.

4. We multiply the dipole response with the Gaussian of the frequency domain in order to get the response of the whole chain to the Gaussian, as we solved the system for a continuous width excitation in the previous step.

5. We perform the Fourier transform of all dipole moments back to time domain in order to get the response of the chain in time domain, which is the result of interest.

3.2.1 Fourier transform

In this subsection we will describe the Fourier transforms and the algorithm we will use to calculate them. First of all, we choose a Gaussian in the time domain, corresponding to our laser pulse.

$$\vec{E_g}(t) = \vec{E}_0 e^{-i\omega_0 t - \left(\frac{t-t_0}{\Delta t}\right)^2} \tag{3.2}$$

Here $\vec{E}_0$ is the amplitude of the gaussian electric field, which is given in arbitrary units. The Gaussian pulse is centered around $t = t_0$ in time domain and it has a duration of Δt, which is also the standard deviation of the Gaussian. The Fourier transforms relating time and frequency domain are very useful in physics; in the following lines we will remember their expressions.

$$F(\omega) = \frac{1}{\sqrt{2\pi}} \int_{-\infty}^{\infty} f(t) e^{i\omega t}\, dt \tag{3.3}$$

$$f(t) = \frac{1}{\sqrt{2\pi}} \int_{-\infty}^{\infty} F(\omega) e^{-i\omega t}\, d\omega \tag{3.4}$$

Following equation 3.3 we get the Fourier transform of 3.2

$$\vec{E_g}(\omega) = \frac{\vec{E}_0 \Delta t}{\sqrt{2}} e^{i(\omega-\omega_0)t_0 - \left(\frac{(\omega-\omega_0)\Delta t}{2}\right)^2} \tag{3.5}$$

This function is a propagating Gaussian, now centered at frequency ω_0 and with a width of $\Delta\omega = 2/\Delta t$; therefore, if we choose a narrow pulse in the time domain, we will obtain a wide Gaussian in the frequency domain, and vice versa. Since we already have defined both Gaussians, we can proceed with the calculation of the chain's modes.

We will analyse now the response of the chain in the frequency domain. When we have calculated $\vec{p}_n(\omega)$ for each particle, we will multiply it with the frequency domain Gaussian for all frequencies, in order to get the response to the pulse in this domain:

$$\hat{p}_n(t) = \vec{E_g}(\omega) \cdot \vec{p}_n(\omega),\ n = 1, 2, \ldots, N \tag{3.6}$$

Finally, we will transform the chain's response to time domain using equation 3.4:

$$\hat{p}_n(\omega) = \frac{1}{\sqrt{2\pi}} \int_{-\infty}^{\infty} \vec{p}_n(\omega) e^{-i\omega t}\, d\omega \tag{3.7}$$

3.2.2 Gaussian parameters

In this brief section the values of the parameters chosen for the Gaussian pulse are introduced. All parameters will be invariant throughout this report except for the central frequency ω_0, so that different modes of the chain can be excited.

- $\vec{E} = 1$, the amplitude of the Gaussian, given in arbitrary units []a.u.].
- $t_0 = 200$ [fs], central time of the Gaussian in time domain, where the amplitude reaches its maximum.
- $\Delta t = 80$ [fs], the width of the pulse in time-domain. From its corresponding width in frequency domain, $\Delta\omega = 2/\Delta t$, we can determine which other modes around the central frequency are excited, so that a small value of $\Delta\omega$, or, in another words, a large value of Δt, will give a sharp distribution function, so that only few modes will be excited. In our simulations, $\Delta\omega = 0.025$ (rad/fs).
- ω_0, the central frequency lies in a range of $\omega_0 = 3.9$-4.6 (rad/fs) for longitudinal polarization and $\omega_0 = 3.5$-4.2 (rad/fs) for transversal polarization. We know previous calculations so that plasmonic modes will be excited within these ranges.

3.2.3 Algorithm

To conclude this chapter we will precise a couple of details about the Fourier transform. In this reseach we have used a numerical Fourier transform called Fast Fourier Transform (FFT), which is an intrinsic function of MATLAB. Since the resolution was good enough, we have chosen to use this method because it is much faster. This method uses the Discrete Fourier transform; however, describing this method is not of our concern here: more information can be easily found in the *help* command of MATLAB [21].

Finally we introduce the relation between the time and frequency in this kind of numerical computations. If $d\omega$ is the frequency step in the frequency grid, and there are N_{grid} points in the frequency grid, the time step of the Fourier transform is given by:

$$dt = \frac{2\pi}{d\omega \cdot N_{grid}} \tag{3.8}$$

Chapter 4

Results

The necessary theory has been given and developed in the 2nd chapter, while the methods have been described in the previous chapter; so it is time now to look at the results of this simulation. The main goal of this project is to look at the influence of losses in the wave-guiding properties of the chain, i.e. in the propagation of the plasmonic modes. The material we are using is silver, and from the experimental fits of references [9] and [10], the damping factor is $\gamma_1 = 0.0835$ (PHz), as introduced in equation 3.1. In this chapter we will consider this value (from now on it will be labeled as γ_1), and we will also take its double, $\gamma_2 = 0.167$ (PHz). Damping factor γ is proportional to the lifetime of the plasmon, which is inversely proportional to the imaginary part of the angular frequency of the excited mode. Therefore, we expect a smaller lifetime of the plasmon for bigger damping γ_2.The response of the excitation of the chain will be compared for both values, and the same will be done for the dispersion relation. To conclude this chapter, plasmons will be analysed from the point of view of energy transport .

4.1 First overview

In this chapter the first results will be shown to give a taste of what we expect. Our main interest lies on the comparison between the response considering γ_1 and γ_2. The difference between them can be seen in the polarizability of the silver nanoparticles. Drude's model for polarizability takes the Ohmic damping into account by introducing γ factor, as we have seen in equation 2.46. Therefore, a system with γ_2 has larger losses than that with γ_1 (remember $\gamma_2 > \gamma_1$). The absolute value of the polarizability is shown below for both γ_1, γ_2.

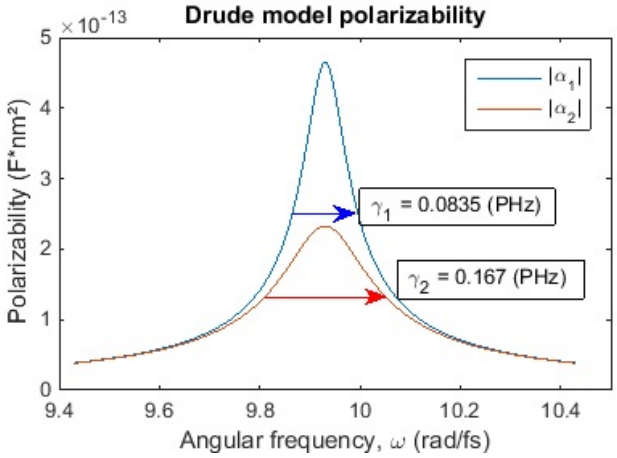

Figure 4.1: Polarizability calculated using Drude's model, plotted for $\gamma_1 = 0.0835$ (PHz) and $\gamma_2 = 0.167$ (PHz).

According to Drude's model, the shape of the polarizability in frequency domain is a Lorentzian,

as it is clearly seen in figure 4.1. The plot corresponding to larger γ_1 is broader than that of γ_2, so the polarizability for bigger damping factor yields lower values. Since this magnitude affects quantities such as electric dipole moments, as seen in equations 2.1 and 2.2, a different behaviour for both cases is expected. Further results concerning plasmon propagation for different γ values will be shown later.

Besides, we also expect to have different results for different polarizations, longitudinal and transversal, since the equations presented in chapter 2 make a difference between them. In order to somehow anticipate the results, we have plotted in figure 4.2 the response of the chain for central frequency $\omega_0 = 4.0$ and γ_1 for the two polarizations.

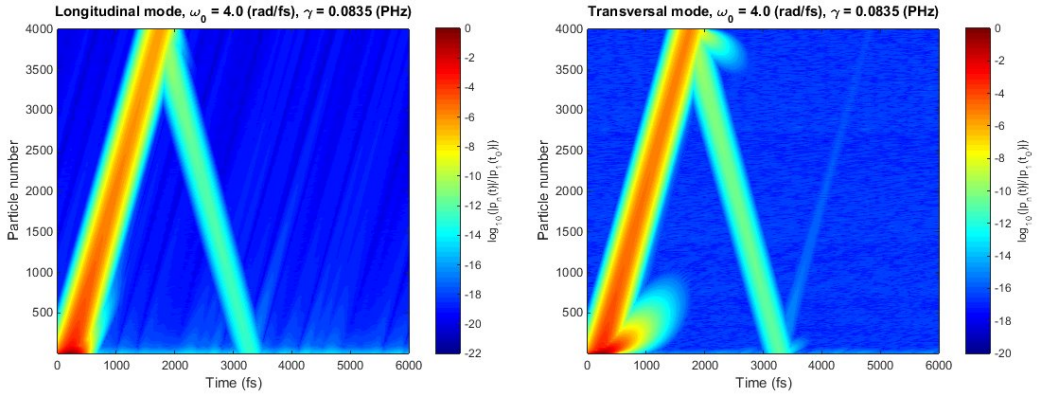

Figure 4.2: Logarithm of the absolute value of electric dipole moments normalized with respect to the dipole moment of the first particle at $t = t_0$ as a function of time, in a chain of 4000 silver nanoparticles of radius $a = 25$nm and nearest-neighbour distance $d = 75$nm, with damping factor $\gamma_1 = 0.0835$ (PHz), for longitudinal and transversal polarizations. Only the first particle is excited with a Gaussian of central frequency $\omega_0 = 4.0$ (rad/fs).

In figure 4.2 we plot the normalized dipole moments of the particles in the chain with respect to the dipole moment of the first particle at $t = t_0$ as a function of time. For both polarizations contours show a main signal propagating along the chain with decreasing amplitude until it is lost. Since it is a straight line, it has a constant velocity. When this propagation reaches the last particle of the chain (N = 4000), it is reflected, and the pattern repeats itself with lower intensity, due to the losses in the propagation. However, this signal vanishes earlier in the longitudinal case, as it can be seen comparing the intensity of the colours in the scales. On the other hand, there is a tiny signal propagating near this main signal at the beginning of the chain. In both cases its velocity is smaller than the other signal, and it also vanishes faster, both in time and space. Besides, this second mode is slower in the transversal case, but it propagates during a longer time period. The first signal we have described is called a *forerunner*, also named as *precursor*. The front of a propagating wave sees no oscillations of electrons in the nanoparticles, so the effective medium through which it propagates is not affected by any extra motion: the dielectric permitivitty $\epsilon(\omega)$ is constant at $\omega = 0$ (equation 2.11). Therefore, it travels through the chain at the speed of the light in the medium. This is easily verified by calculating the slope of the line from figure 4.2: a velocity of $v = 199.8$ (nm/fs) is obtained, which matches the speed of light in glass, c/n, where $n = 1.5$. The amplitude of the signal decays in space and time, so it is affected by loses. The second and smaller signal is the *surface plasmon*, and this is the propagating mode we are looking at. Its behaviour is different in longitudinal and transversal polarizations: the propagating velocity and propagating length are not the same. The plasmon in the longitudinal mode has a higher speed, but the signal is narrower, so it decays faster in time. The transversal plasmon is slower at the same frequency, but it vanishes later in time. Therefore, different polarizations show different plasmonic modes which are affected by losses in diverse ways, as it can be seen from the velocity and the propagation length. The effects and influence of losses in plasmon propagation will be presented in more detail in the following chapter

4.2 Response of the chain to the pulse excitation

4.2.1 Longitudinal polarization

In this subsection the calculations for the response of the chain in the longitudinal polarization are presented. We remind that the chain consists of 4000 particles, with $d = 75$nm between a pair of particles, whose axis is parallel to the $\hat{x}$-direction. We consider a limited time-period in which the propagation of plasmonic modes happens before they completely decay. Since the we are studying the effect of losses in plasmons, calculations are done considering damping factors $\gamma_1 = 0.0835$ (PHz) and $\gamma_2 = 0.167$ (PHz), which stand for Ohmic losses in the Drude model. The first particle of the chain is excited by a pulse, and the resulting response of the chain is analysed within the range $\omega_0 = 3.9$-4.6 (rad/fs) for central frequencies of the Gaussian, where we expect to excite different plasmonic modes. This response is plotted along the particles in the chain as a function of time in figures 4.3 and 4.4.

From this profiles many interesting features can be deduced. The first one is that, for frequencies around $\omega_0 = 4.0 - 4.1$, there is a plasmon overlapping with the forerunner, which means that their propagating velocities are very similar. Due to this, it is complicated to distinguish between them. For the rest of the frequencies, we suggest that the propagation velocities for both damping coefficients are nearly the same, since their shape and slope with respect to distance and time seems to be very similar. The main difference comes from the propagation length: for γ_2 the plasmon decays faster, so the travelled distance is shorter under this condition. This is also related to the lifetime of the plasmonic mode, which is shorter for bigger damping, and it is inversely proportional to the imaginary part of the frequency. In order to determine mentioned quantities such as velocity, we will plot the time profiles of the contour: how the normalized dipole moments evolve as a function of distance at given times. These profiles, presented in figures 4.5 and 4.6, will be very useful in order to track our propagating modes.

Comparing figures 4.5 and 4.6 to 4.3 and 4.4 respectively, it is easy to identify both the forerunner and the plasmon: The wider and nearly constant propagating peak is the forerunner, while the sharper and fastly decaying peaks, depending on the central frequencies, are profiles of the plasmon. The comparison between columns show that for γ_2, i.e. for bigger losses, the plasmon intensity decays faster, and the propagation length is also shorter. By tracking the second peak, we are able to calculate the propagation velocity and the decay, related to the lifetime of the plasmon. Plotting the position of the peak as a function of time yields the velocity of propagation of the plasmon; while the representation of the normalized dipole moment with respect to time gives its decay factor. Before moving on, note that these profiles also show an interesting characteristic of the forerunners. At central frequencies $\omega_0 = 4.5$ and $\omega = 4.6$, with γ_1 (smaller losses), a secondary peak or shoulder is discernible, which suggests that there are two precursors. In fact, in literature there are two, named Brillouin and Sommerfeld forerunners. Nevertheless, a more detailed analysis is beyond the scope of this project; for more information please check reference [17].

We show some plots of the position of plasmon peaks with respect to time in figure 4.7. From left to right, each column belongs to γ_1 and γ_2. For frequencies around $\omega_0 = 4.0$-4.2 (rad/fs), which is the region in the vicinity of the crossing of light dispersion relation with the dispersion relation of longitudinal modes it has been a difficult task to separate the plasmon and the forerunner, since their velocities are very similar. As a result, those velocities contain bigger errors. Besides, in the same frequency region we see that the line is not straight, as it is the case for the rest of the frequencies, but they are curved. Each line with a different slope corresponds to a certain mode. This means that more than one mode are excited there, coming from the term $\Delta\omega$. The width of the Gaussian enables to excite modes not only with frequency ω_0, but those modes whose frequency lies within range $\omega_0 \pm \Delta\omega$. The thin red line is the linear fit of the plot. Looking at the effect of losses, the shape of lines is very similar for both γ_1 and γ_2. When it comes to velocities, the measured quantities are very different in the region around the light line, while the match is good away from that region. Calculated quantities will be shown in the next section, comparing with the group velocities (figures 4.22 and 4.23).

To conclude this subsection, we plot the magnitude of plasmon peaks as a function of time, in order to determine the decay. Some of those are shown in figure 4.8. Taking the natural logarithm

of the normalized dipoles, the plots show a perfectly linear decreasing slope. This is not surprising, since the dipole moments are harmonic waves with $e^{-i(\omega_r+i\omega_i)t} = e^{-i\omega_r t+\omega_i t}$, as seen in section 2.4.1; therefore, the slope of this lines is the imaginary part of the frequency ω_i. The lifetime of the plasmon is determined from here, as both quantities are inversely proportional, i.e. $\tau = 1/\omega_i$. Comparing the decay of both columns, given by coefficient $m2$, we see that for γ_2 the absolute value of the decay is bigger. This is in accordance with our expectations, since bigger γ means that losses increase, leading to shorter lifetimes. Calculated decays will be shown in the next section, comparing with the results calculated from dispersion relations (figure 4.17).

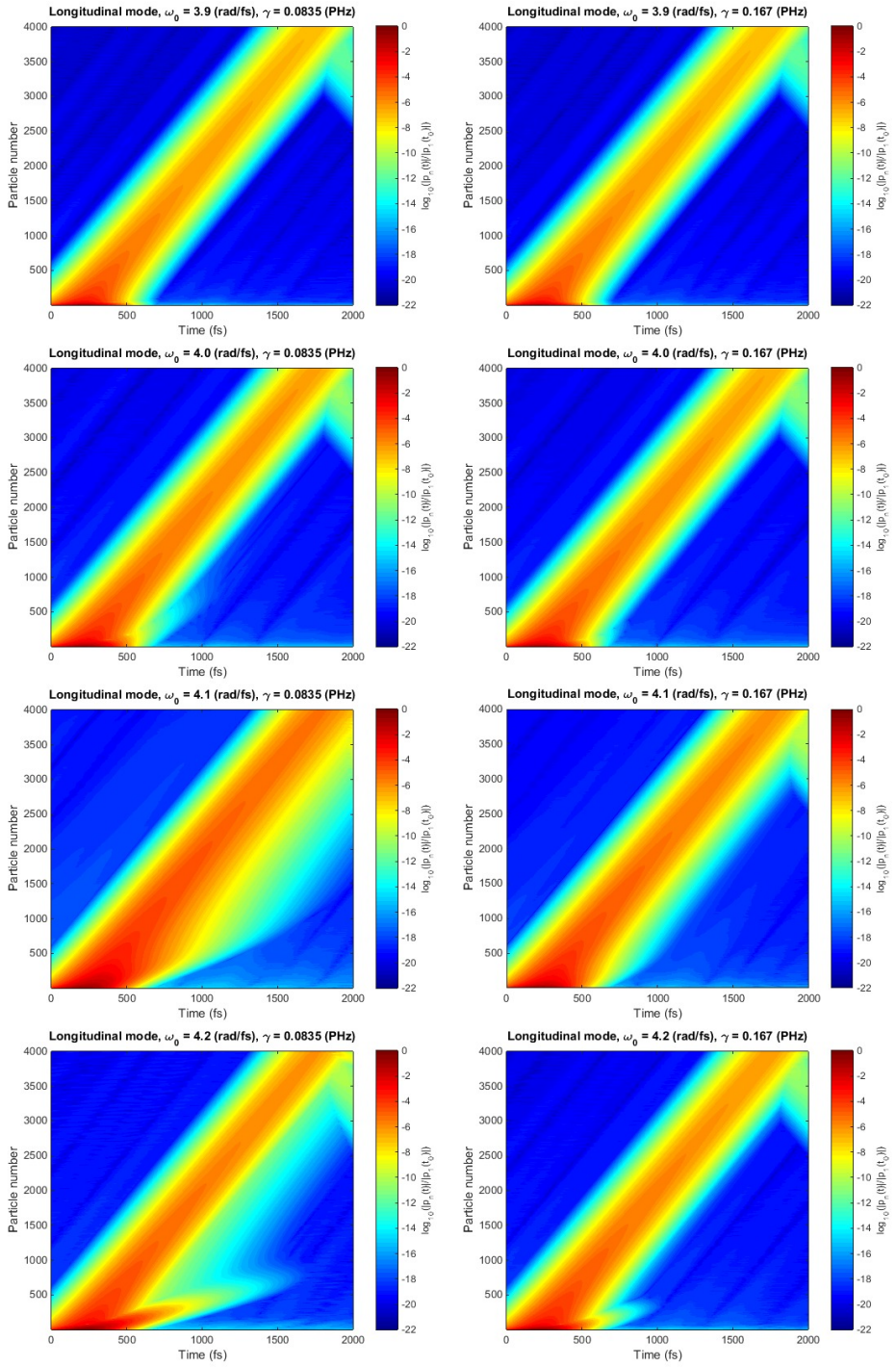

Figure 4.3: Logarithm of absolute value of electric dipole moments normalized with respect to the dipole moment of the first particle at $t = t_0$ as a function of time in a chain of 4000 silver nanoparticles, for central frequencies ω_0 = 3.9-4.2 (rad/fs), with $\Delta\omega = 0.025$ (rad/fs) and longitudinal polarization. On the left column, plots for $\gamma_1 = 0.0835$ (PHz); on the right, results for $\gamma_2 = 0.167$ (PHz), i.e. simulations with bigger losses.

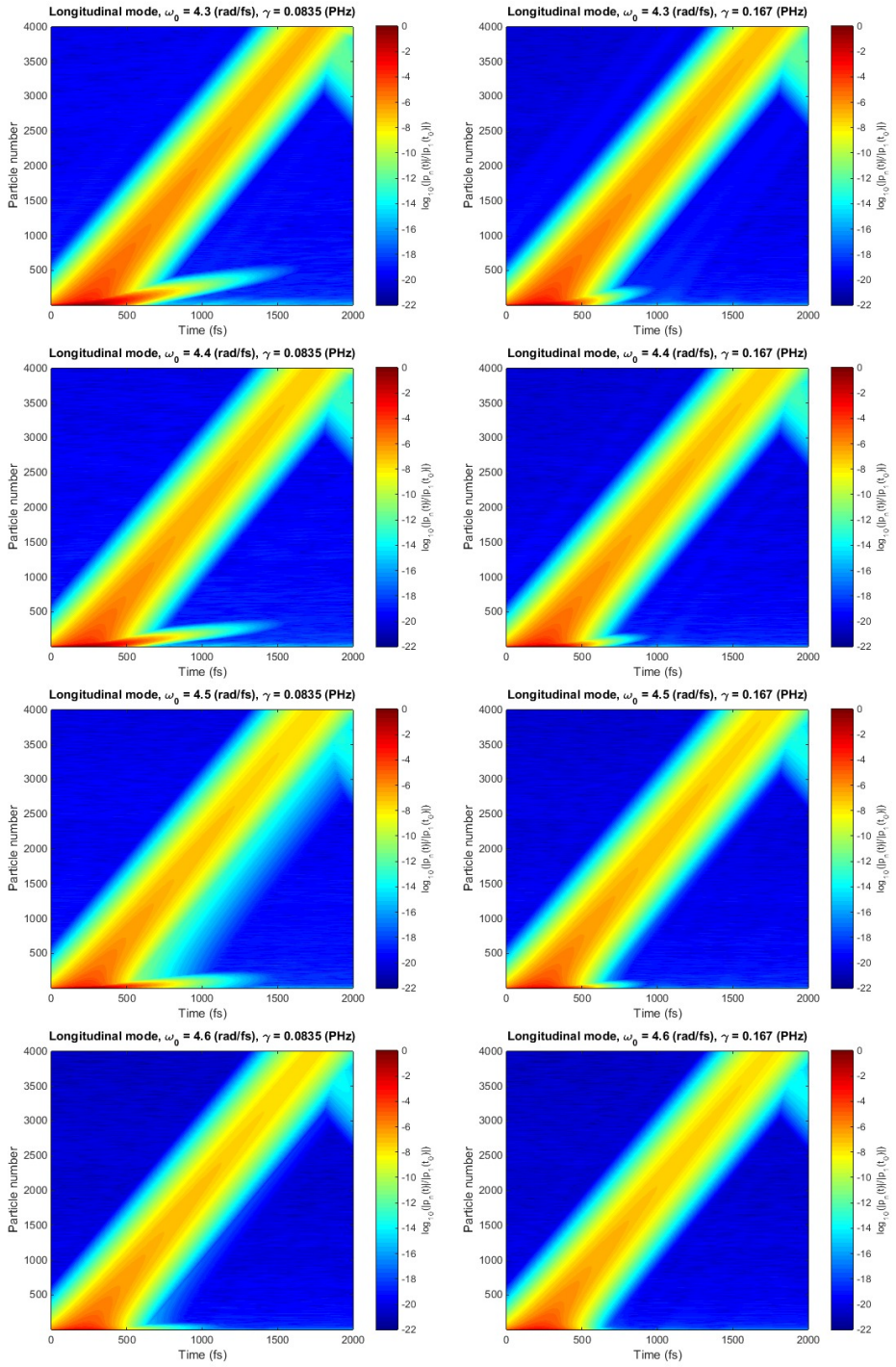

Figure 4.4: Logarithm of the absolute value of electric dipole moments normalized with respect to the dipole moment of the first particle at $t = t_0$ as a function of time in a chain of 4000 silver nanoparticles, for central frequencies $\omega_0 = 4.3$-4.6 (rad/fs), with $\Delta\omega = 0.025$ (rad/fs) and longitudinal polarization. On the left column, plots for $\gamma_1 = 0.0835$ (PHz); on the right, results for $\gamma_2 = 0.167$ (PHz), i.e. simulations with bigger losses.

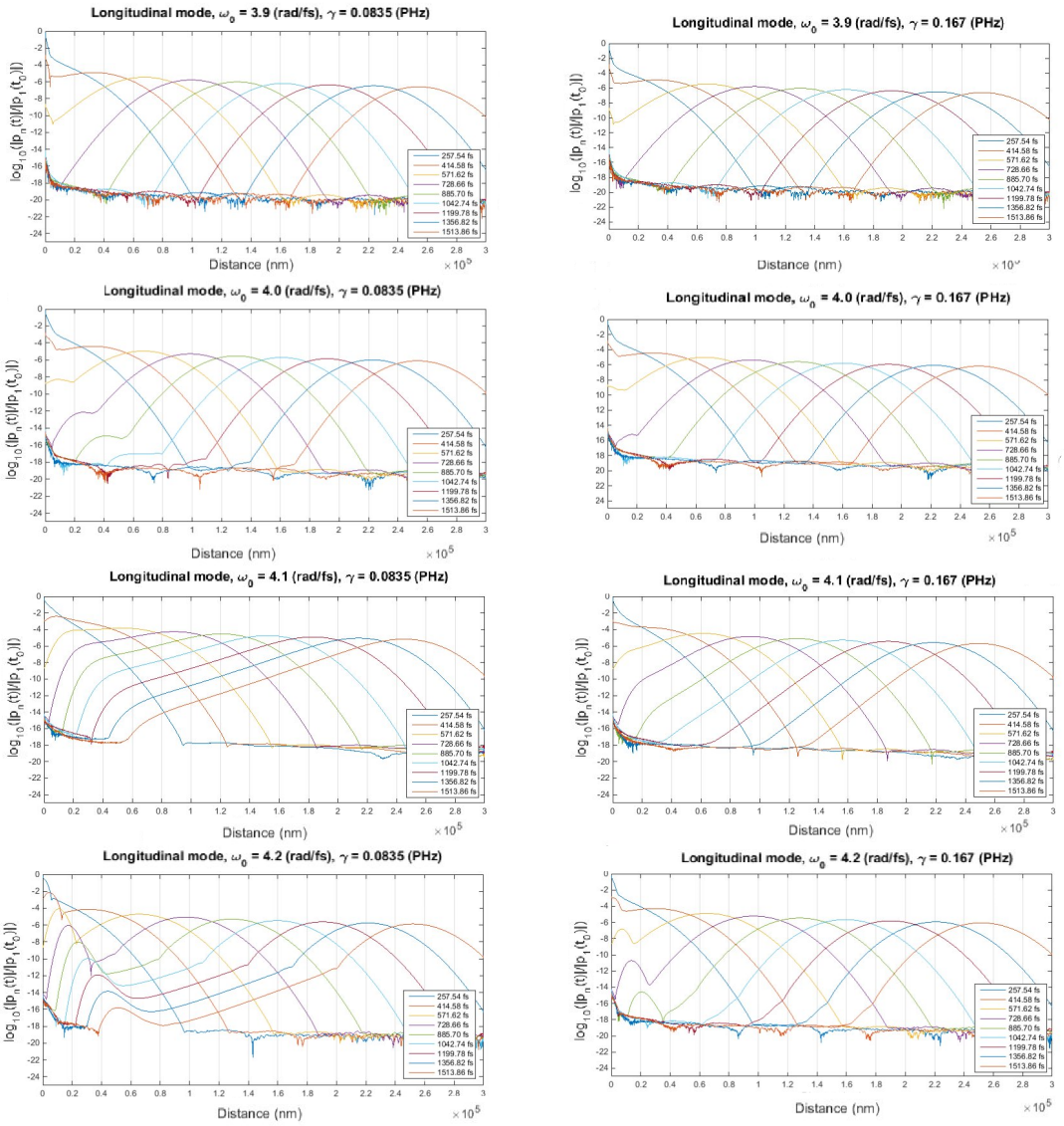

Figure 4.5: Logarithm of the absolute value of electric dipole moments normalized with respect to the dipole moment of the first particle at $t = t_0$ as a function of distance, plotted at different times, in a chain of 4000 silver nanoparticles, for central frequencies ω_0 = 3.9-4.2 (rad/fs), with $\Delta\omega = 0.025$ (rad/fs) and longitudinal polarization. On the left column, plots for $\gamma_1 = 0.0835$ (PHz); on the right, results for $\gamma_2 = 0.167$ (PHz), i.e. simulations with bigger losses.

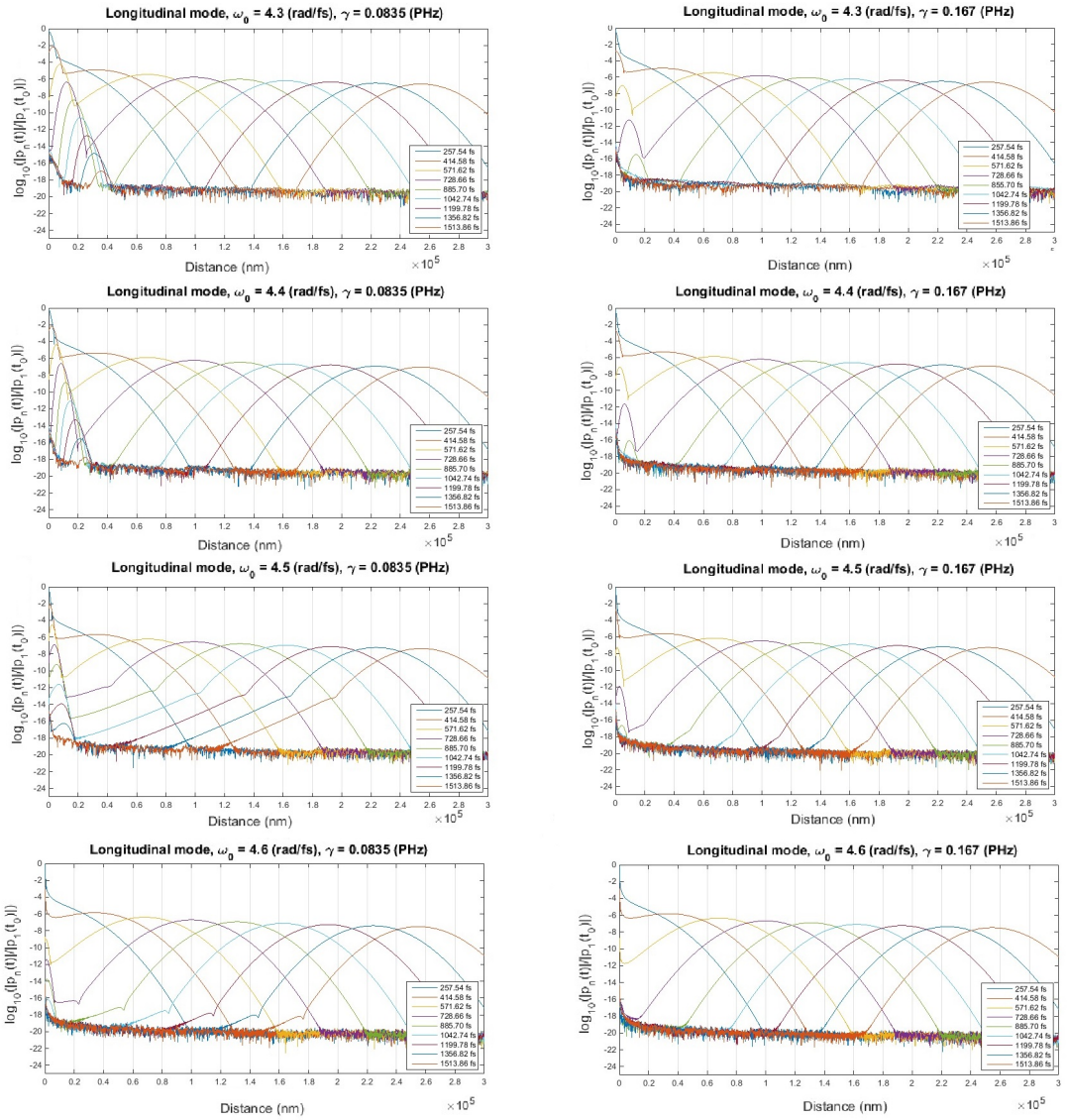

Figure 4.6: Absolute value of electric dipole moments normalized with respect to the dipole moment of the first particle at $t = t_0$ as a function of distance, plotted at different times, in a chain of 4000 silver nanoparticles, for central frequencies $\omega_0 = 4.3$-4.6 (rad/fs), with $\Delta\omega = 0.025$ (rad/fs) and longitudinal polarization. On the left column, plots for $\gamma_1 = 0.0835$ (PHz); on the right, results for $\gamma_2 = 0.167$ (PHz), i.e. simulations with bigger losses.

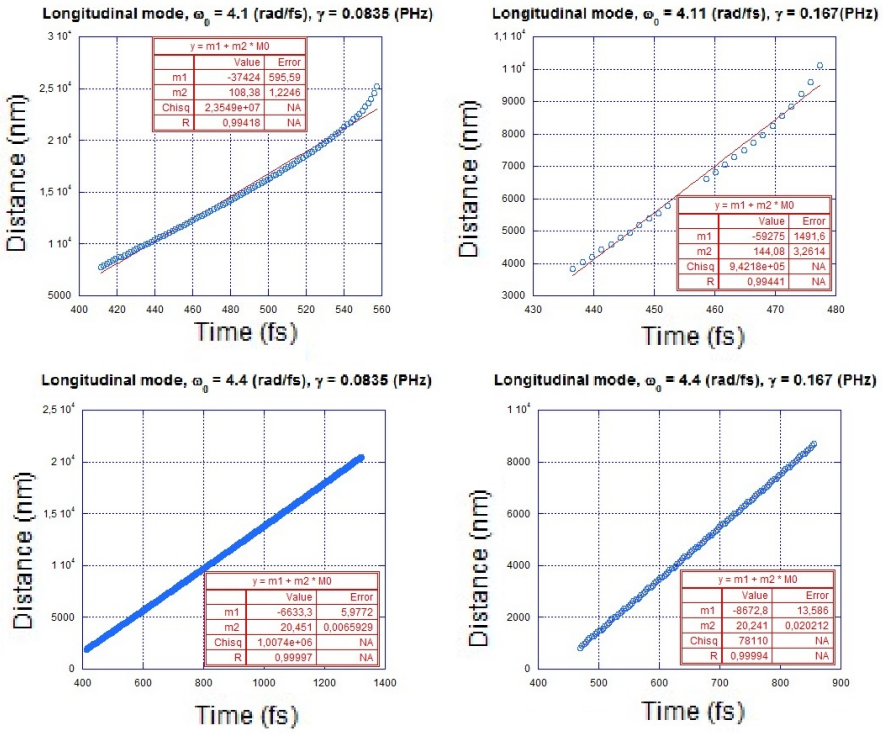

Figure 4.7: Propagation of longitudinal modes of a chain with 4000 particles as a function of time at $\omega_0 = 4.1/4.11$ and 4.4 (rad/fs), with width $\Delta\omega = 0.025$ (rad/fs) and longitudinal polarization. On the left column, plots for $\gamma_1 = 0.0835$ (PHz); on the right, results for $\gamma_2 = 0.167$ (PHz), i.e. simulations with bigger losses.

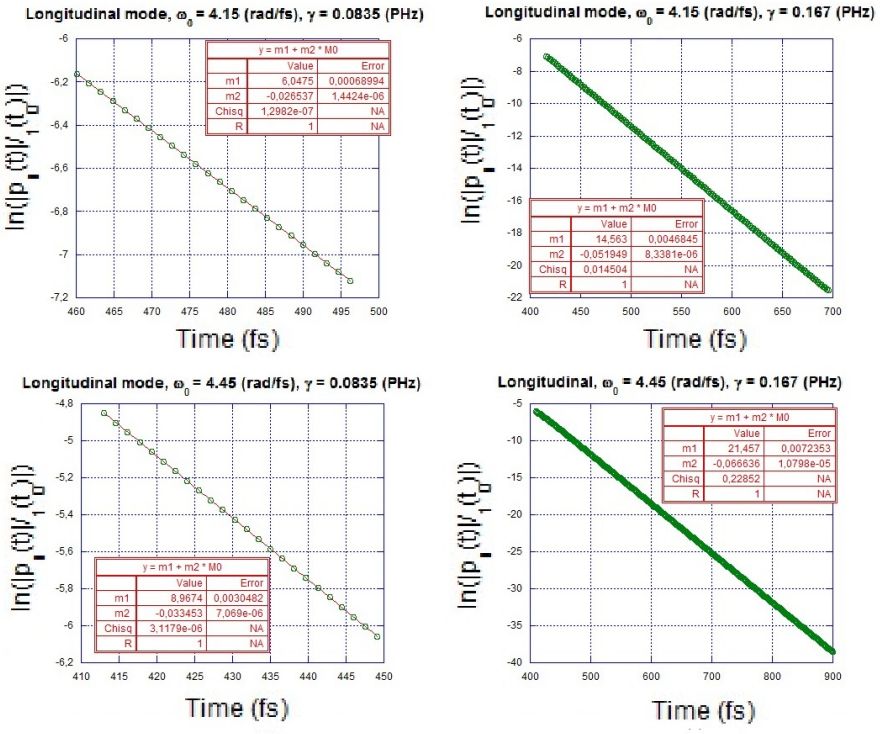

Figure 4.8: Natural logarithm of normalized dipole moments of longitudinal modes of a chain with 4000 particles as a function of time at $\omega_0 = 4.15$ and 4.45 (rad/fs), with width $\Delta\omega = 0.025$ (rad/fs) and longitudinal polarization. On the left column, plots for $\gamma_1 = 0.0835$ (PHz); on the right, results for $\gamma_2 = 0.167$ (PHz), i.e. simulations with bigger losses.

4.2.2 Transversal polarization

In this subsection same quantities as for longitudinal polarization will be shown, but calculated for the transversal polarization. The analysis will be done in the same way: first we show the normalized dipole moments in space and time, then their time profiles, and finally some plots of propagation and signal decay in time. Again, to check the effects of the increase in losses, results for γ_1 and γ_2 will be shown together, and compared with each other.

It is wise to begin by showing the normalized dipole moments in time and space in the frequency range $\omega_0 = 3.5$-4.2 (rad/fs) in figures 4.9 and 4.10. Note that this range is different from the range of the longitudinal mode: this shows that each polarization has different modes. The rest of the parameters are the same, and the response is also similar. We can see a forerunner and a plasmon in the excited frequencies. At the lowest frequencies of the range both have similar velocities, and at higher frequencies propagation velocity and length decrease for the plasmon. Looking at the losses, it is clear that the propagation length and normalized dipole moment decay faster for γ_2 than for γ_1. At this point, we observe that comparing the transversal plots for each γ_1, γ_2 with their longitudinal counterparts, the plasmon decays faster in the longitudinal case. This can be stated looking at the contours, where the plasmons in the transversal polarizations (figures 4.9 and 4.10) are wider in space and time in the longitudinal case (figures 4.3 and 4.4). Therefore, even though same γ factors are considered, it is concluded that losses for transversal polarization are smaller than those in the longitudinal polarization. We will analyse this later in the section corresponding to dispersion relations.

Time profiles are plotted in figures 4.11 and 4.12. In these profiles forerunners and plasmons are easily distinguishable. Therefore, we can track the position and normalize dipole moment of the plasmon peak in time to get propagation velocities and decays for each mode; some graphs for those calculations are shown in figures 4.13 and 4.14. Looking at the propagation of forerunners, we can see the structure suggesting two precursors at $\omega_0 = 4.0$ (rad/fs), γ_1 plot and at $\omega_0 = 4.1$ (rad/fs) for both γ_1,γ_2. Note that in the longitudinal case we did not observe this structure in any plot with γ_2 (figures 4.5 and 4.6). Nevertheless, we will not study the behaviour of forerunners any further.

We will end section describing the behaviour of the position and amplitude corresponding the plasmonic peak as a function of time in figures 4.13 and 4.14.

In figure 4.13 we can see the position of the plasmon peak as a function of time. Presented plots show a straight line, a wavy line and two curved lines. We attribute the waviness of the line to numerical effects of calculations, while it has been stated before that the different modes come from the $\Delta\omega$ term, which allows to excite modes close to the central frequency ω_0. An averaged line is represented by the thin red line. Calculated velocities will be shown together with the group velocities derived from the dispersion relation (figures 4.25 and 4.26). Finally, the decay of the plasmonic peak's amplitude is displayed by plotting the natural logarithm of the normalized dipole moment of the propagating plasmon as a function of time. Analogously to the longitudinal case (figure 4.8), decreasing lines are obtained. Besides, the absolute value of the slopes for γ_2 are bigger than for γ_1, leading to the enhancement of the absolute value of the imaginary part corresponding to the mode, which is a negative quantity, since it is related to the decay of the mode. Measured quantities will be shown in figure 4.20.

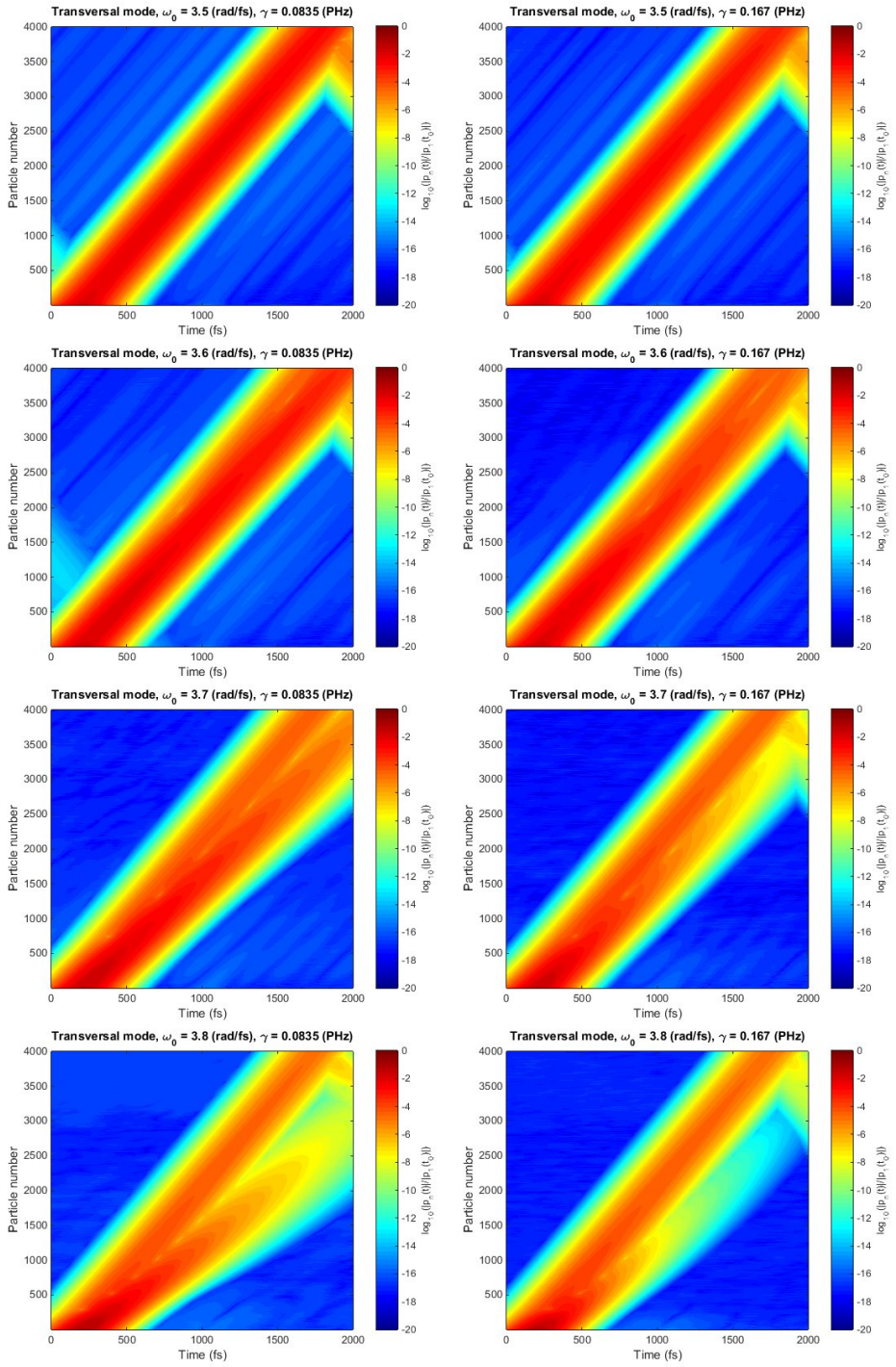

Figure 4.9: Logarithm of the absolute value of electric dipole moments normalized with respect to the dipole moment of the first particle at $t = t_0$ as a function of time in a chain of 4000 silver nanoparticles, for central frequencies ω_0 = 3.5-3.8 (rad/fs), with $\Delta\omega = 0.025$ (rad/fs) and transversal polarization. On the left column, plots for $\gamma_1 = 0.0835$ (PHz); on the right, results for $\gamma_2 = 0.167$ (PHz), i.e. simulations with bigger losses.

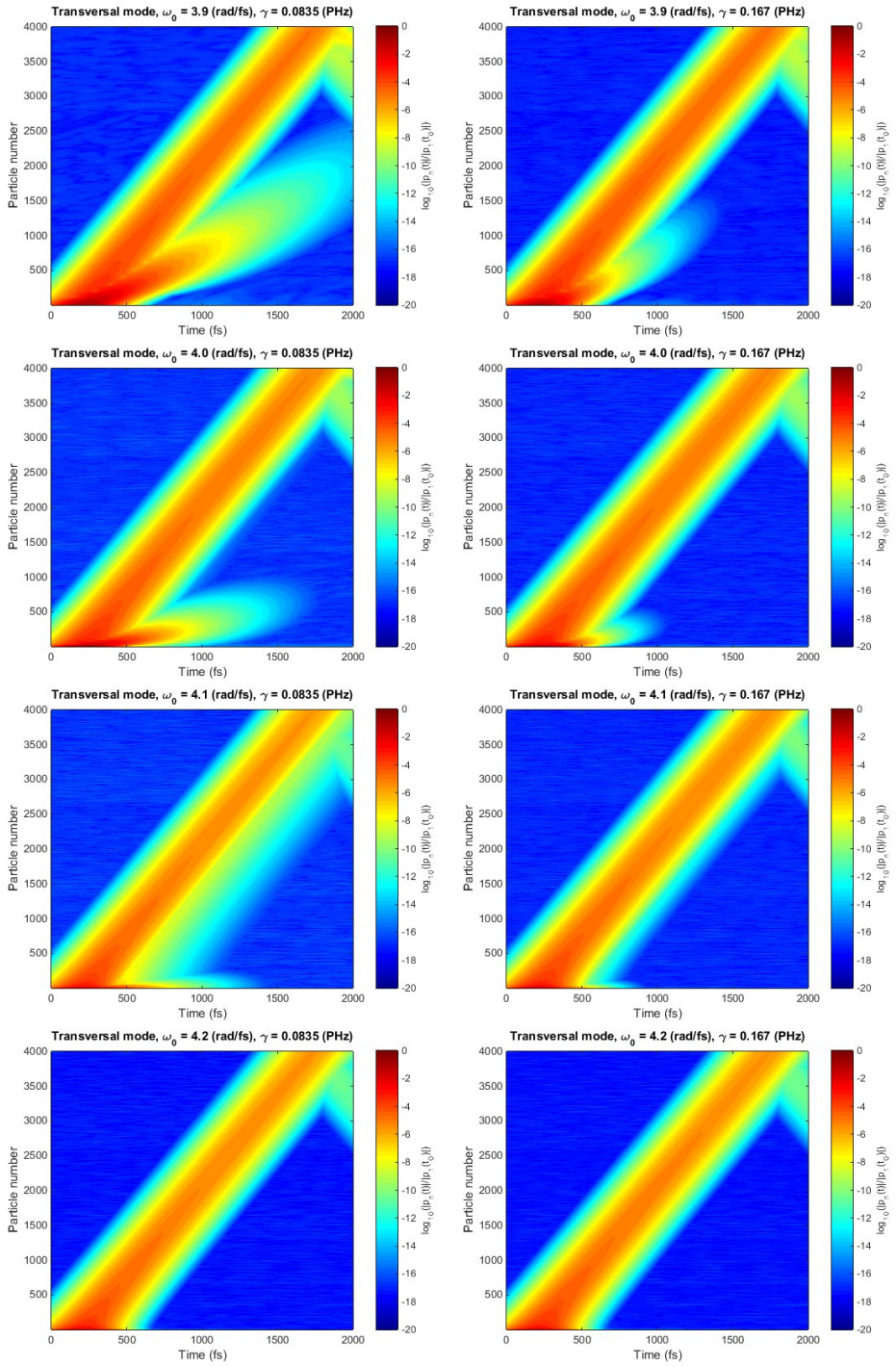

Figure 4.10: Logarithm of the absolute value of electric dipole moments normalized with respect to the dipole moment of the first particle at $t = t_0$ as a function of time in a chain of 4000 silver nanoparticles, for central frequencies $\omega_0 = 3.9$-4.2 (rad/fs), with $\Delta\omega = 0.025$ (rad/fs) and transversal polarization. On the left column, plots for $\gamma_1 = 0.0835$ (PHz); on the right, results for $\gamma_2 = 0.167$ (PHz), i.e. simulations with bigger losses.

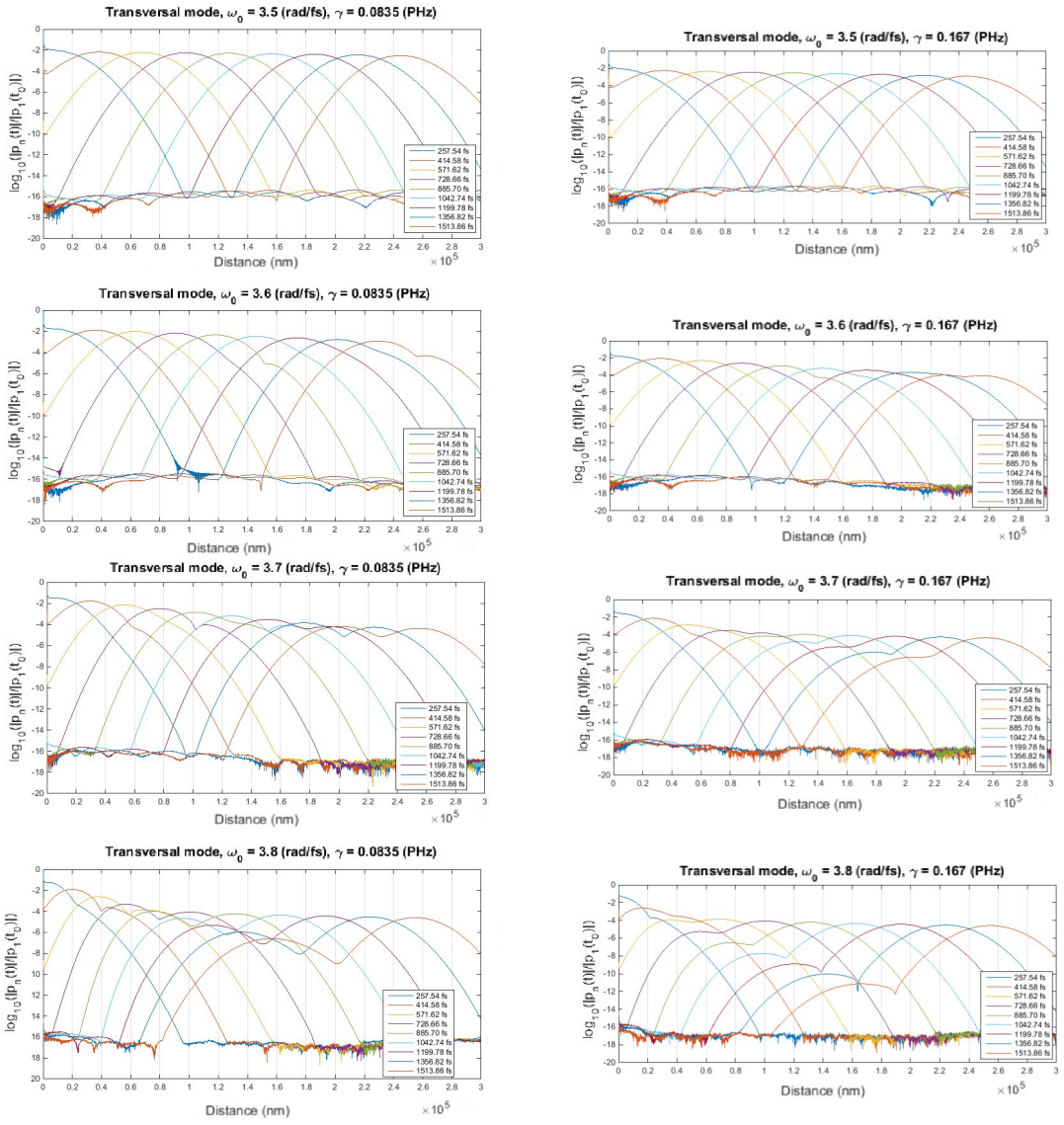

Figure 4.11: Logarithm of the absolute value of electric dipole moments normalized with respect to the dipole moment of the first particle at $t = t_0$ as a function of distance, plotted at different times, in a chain of 4000 silver nanoparticles, for central frequencies ω_0 = 3.5-3.8 (rad/fs), with $\Delta\omega$ = 0.025 (rad/fs) and transversal polarization. On the left column, plots for γ_1 = 0.0835 (PHz); on the right, results for γ_2 = 0.167 (PHz), i.e. simulations with bigger losses.

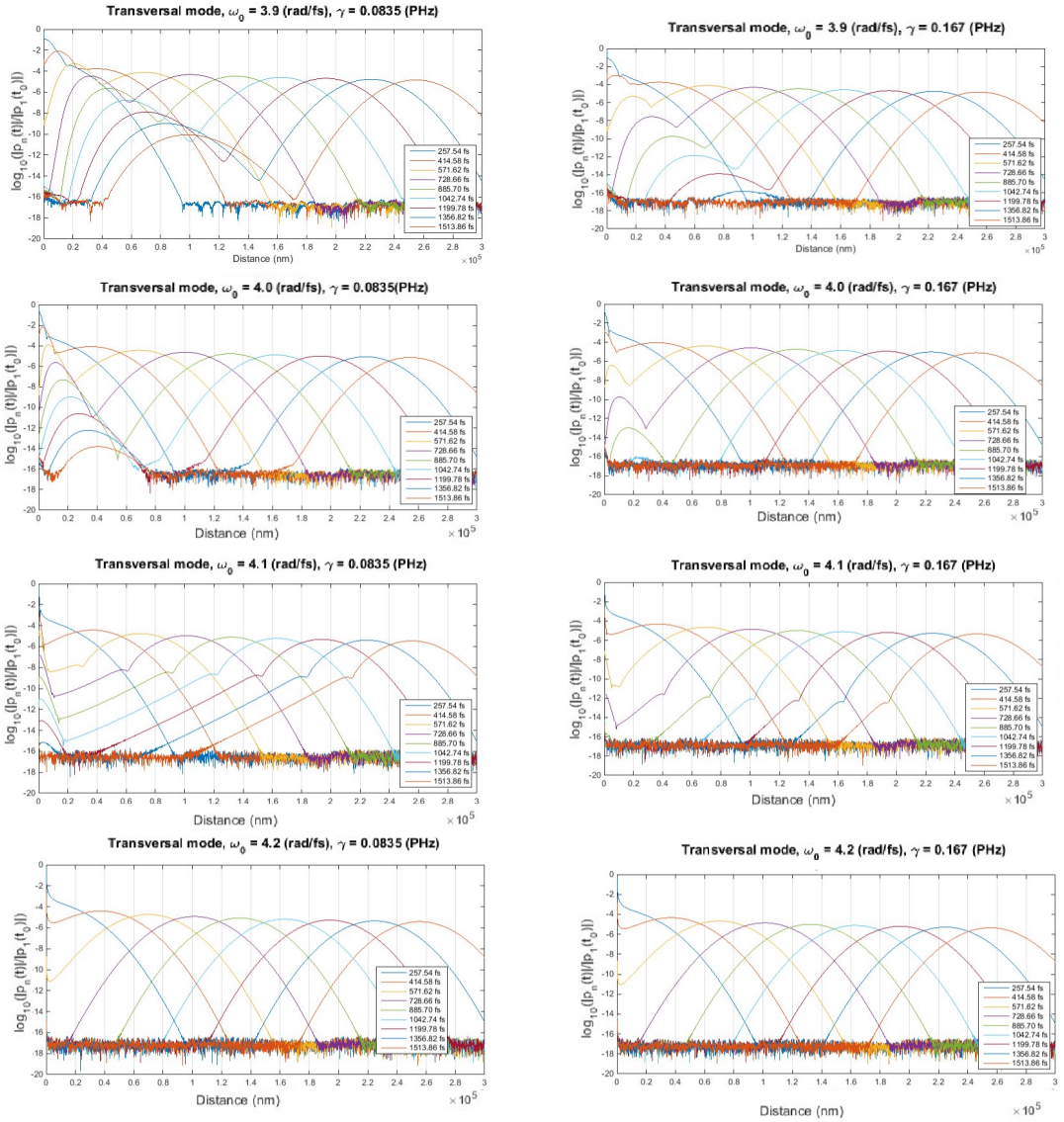

Figure 4.12: Logarithm of the absolute value of electric dipole moments normalized with respect to the dipole moment of the first particle at $t = t_0$ as a function of distance, plotted at different times, in a chain of 4000 silver nanoparticles, for central frequencies ω_0 = 3.9-4.2 (rad/fs), with $\Delta\omega$ = 0.025 (rad/fs) and transversal polarization. On the left column, plots for γ_1 = 0.0835 (PHz); on the right, results for γ_2 = 0.167 (PHz), i.e. simulations with bigger losses.

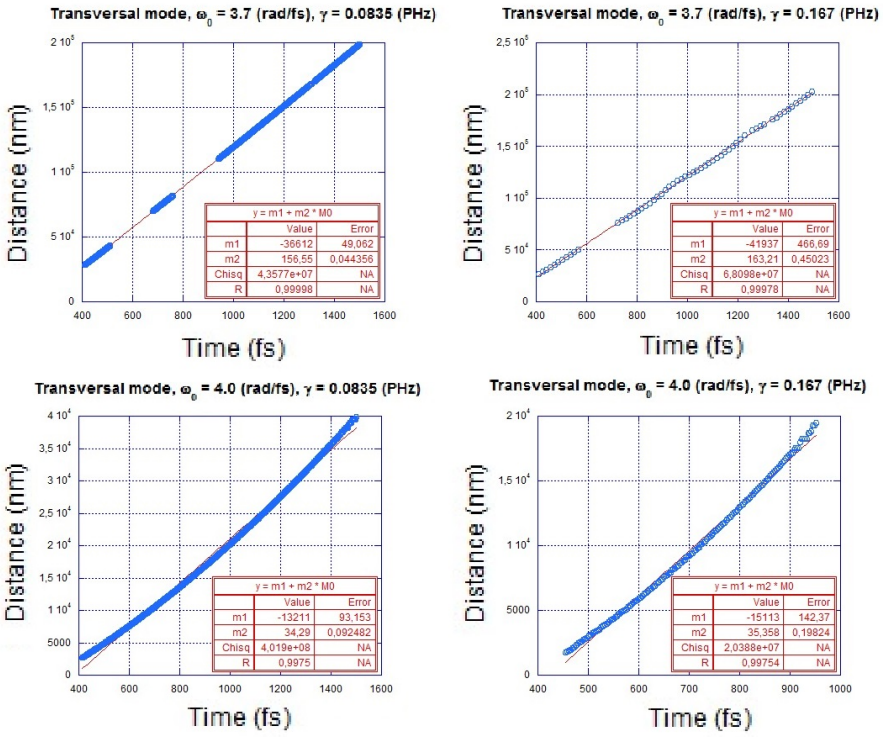

Figure 4.13: Propagation of transversal modes of a chain with 4000 particles as a function of time at $\omega_0 = 3.7$ and 4.0 (rad/fs), with width $\Delta\omega = 0.025$ (rad/fs) and transversal polarization. On the left column, plots for $\gamma_1 = 0.0835$ (PHz); on the right, results for $\gamma_2 = 0.167$ (PHz), i.e. simulations with bigger losses.

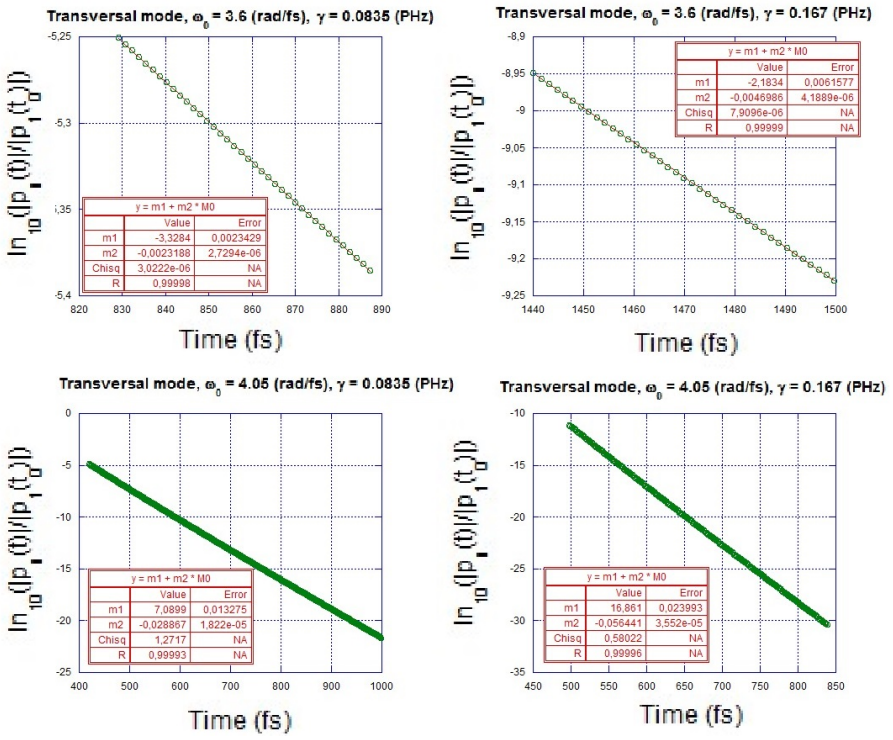

Figure 4.14: Natural logarithm of normalized dipole moments of the transversal modes of a chain with 4000 particles as a function of time at $\omega_0 = 3.6$ and 4.05 (rad/fs), with width $\Delta\omega = 0.025$ (rad/fs) and transversal polarization. On the left column, plots for $\gamma_1 = 0.0835$ (PHz); on the right, results for $\gamma_2 = 0.167$ (PHz), i.e. simulations with bigger losses.

4.3 Dispersion relations

4.3.1 Losses of plasmons

In this section we will use the theory introduced in section 2.4 in order to calculate the dispersion relation for both $\gamma_1 = 0.0835$ (PHz) and $\gamma_2 = 0.167$ (PHz). This time an infinite chain is considered. It has been previously stated that the imaginary part of the modes gives the decay of the mode, and its inverse is the lifetime of the plasmon. For γ_2 shorter lifetime is expected, since the plasmon is more affected by losses. We hope to see this in an increase of the imaginary part of the frequency regardless the polarization of the mode.

4.3.1.1 Longitudinal polarization

The starting point of our analysis on how longitudinal modes are affected by losses is the comparison between the dispersion relations for γ_1 and γ_2. In figure 4.15 we plot the real (image on the left) and imaginary (on the right) parts of the modes separated, each for both values of the damping factor.

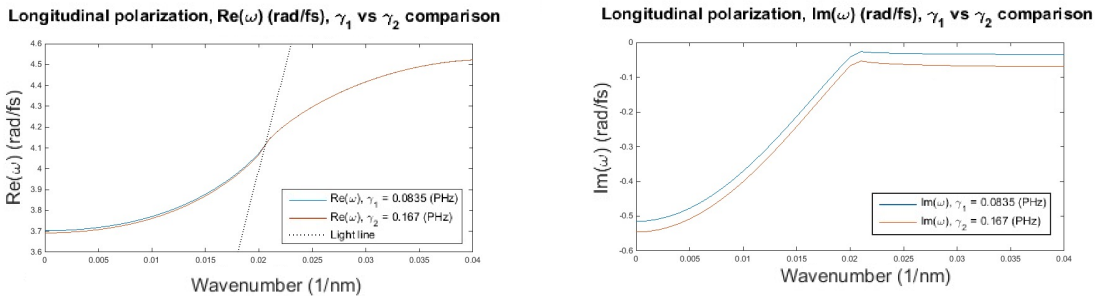

Figure 4.15: Dispersion relation for an infinite chain, real and imaginary part, for both $\gamma_1 = 0.0835$ (PHz) and $\gamma_2 = 0.167$ (PHz), longitudinal polarization.

The figure on the right of 4.15 gives that the real part plots for both γ_1, γ_2 have a very good match: this means that the same modes are excited, so the damping factor does not affect the excited modes. This is in good agreement with figures 4.3 and 4.4, where the same plasmons are seen for different central frequencies ω_0. The difference between modes comes from the propagation length, which is affected by the losses and, therefore, by the imaginary part of the frequency. Again, the right plot in figure 4.15 offers a good explanation for this. The dispersion relation for γ_2 is bigger in terms of absolute value than the line for γ_1, which means that the lifetime of modes with γ_2 is shorter, as expected. Both lines present the same trend: the values are decreasing in the beginning (the plot is given in negative frequencies) and, after reaching a maximum, the absolute value of the imaginary part of frequency increases slightly. The maximum matches the intersection point of the light line with real frequencies, which means that radiative and Ohmic losses are plotted to the left of the maximum, while purely Ohmic losses appear on the right. Note that the lines have similar shapes, but they are displaced with respect to each other, since γ_2 includes more losses than γ_1. In order to clarify this issue, a ratio between the two lines of the imaginary parts is shown in figure 4.16.

We see that after the turning point, i.e. when the real part of the dispersion relation crosses the light line, the ratio of losses increases to 2, which is also the ratio γ_2/γ_1. This means that above the light line losses are not that easy to quantify by varying γ only, while below the light line they are well described by the Drude model, which establishes γ as damping factor, and that losses are purely Ohmic, as expected.

We will finish this subsection by comparing the results obtained from the chain and the dispersion relation. In the previous section we have calculated the decay factor of the amplitude of plasmons by plotting the natural logarithm of the dipole moments as a function of time, as it can be seen in figure 4.8. We claim that these factors are $\omega_i = \mathrm{Im}(\omega)$. Here are the results of this comparison.

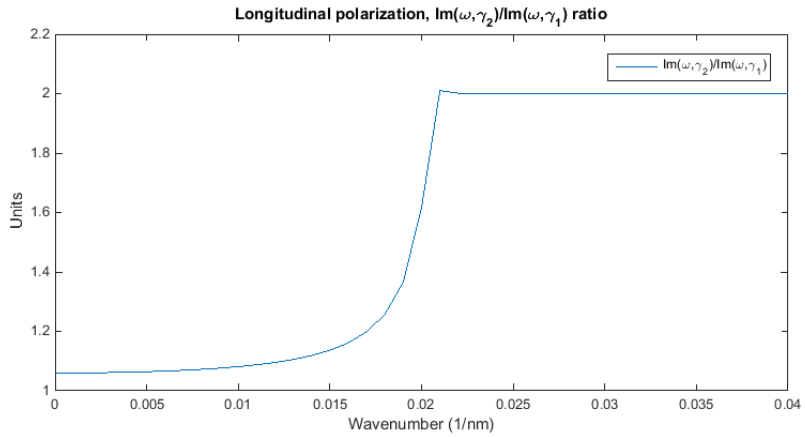

Figure 4.16: $\mathrm{Im}(\omega, \gamma_2)/\mathrm{Im}(\omega, \gamma_1)$ ratio plot for an infinite chain, real and imaginary part, for both $\gamma_1 = 0.0835$ (PHz) and $\gamma_2 = 0.167$ (PHz), longitudinal polarization.

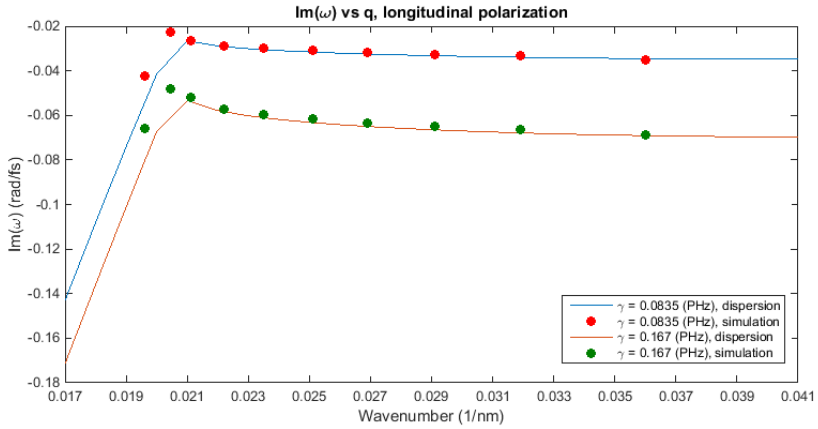

Figure 4.17: Match of the imaginary parts of the frequency obtained from the simulation of the chain's response to the dispersion relations, for $\gamma_1 = 0.0835$ (PHz) and $\gamma_2 = 0.167$ (PHz), longitudinal polarization.

Figure 4.17 shows that the match of the simulations and the imaginary part of the dispersion relation are very accurate in the regime for Ohmic losses, i.e. for wavenumbers bigger than that which matches the dispersion of light. This means that the simulation also give a ratio of $\gamma_2/\gamma_1 \approx 2$ for the losses. We remark that the ratio is approximately 2 because results for lower γ and, consequently, for smaller losses, fits the dispersion relation better. In the region where radiative losses must be included, near the peak in the dispersion relation, we see that the match between the response of the chain and the dispersion relation is not very good. Here radiative losses also play a role, so it can be argued that this is the origin of the mismatch. Besides, the region close to the light line have yielded quite unclear calculations, as it will be shown in the group velocities subsection (4.3.2). Furthermore, it seems that the match for γ_2 is a bit less accurate than that for γ_1, although the difference is not very pronounced.

4.3.1.2 Transversal polarization

The same analysis as for the longitudinal polarization will be conducted here, but for the case of the transversal polarization, considering the infinite chain. The analogous of figure 4.15 will be plotted in 4.18 comparing the dispersion relation for transversal modes evaluated at γ_1 and γ_2.

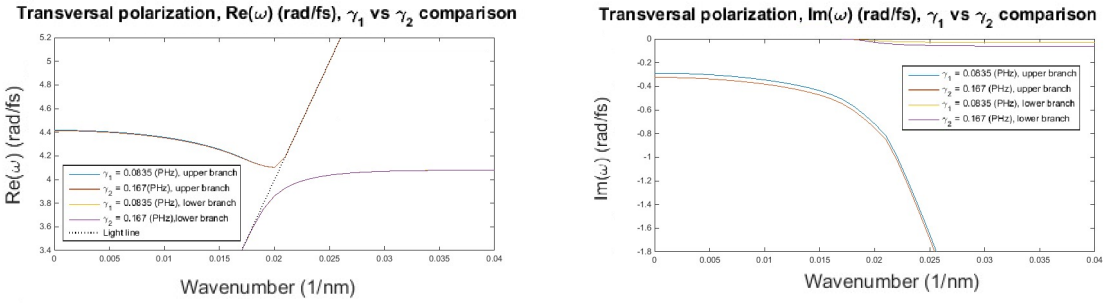

Figure 4.18: Dispersion relation for an infinite chain, real and imaginary part, for both $\gamma_1 = 0.0835$ (PHz) and $\gamma_2 = 0.167$ (PHz), transversal polarization.

Transversal dispersion relation is splitted in two branches: we have modes excited above the light line, and modes excited below the light line. Eventually, modes above the light line match the light line itself, while modes below the line are separated from it. Therefore, we expect for the modes above the line to have both radiative and Ohmic losses, while the damping for modes below the light line are purely Ohmic. Analogously to what happens in figure 4.15, in figure 4.18 the real parts of ω match very well with each other for both damping factors, while for the imaginary part a displacement of the lines can be observed for both upper and lower branches, upper and lower terms referring to the position of real part of the modes with respect to the light line. We calculate the ratio $\mathrm{Im}(\omega, \gamma_2)/\mathrm{Im}(\omega, \gamma_1)$ and show it in figure 4.19.

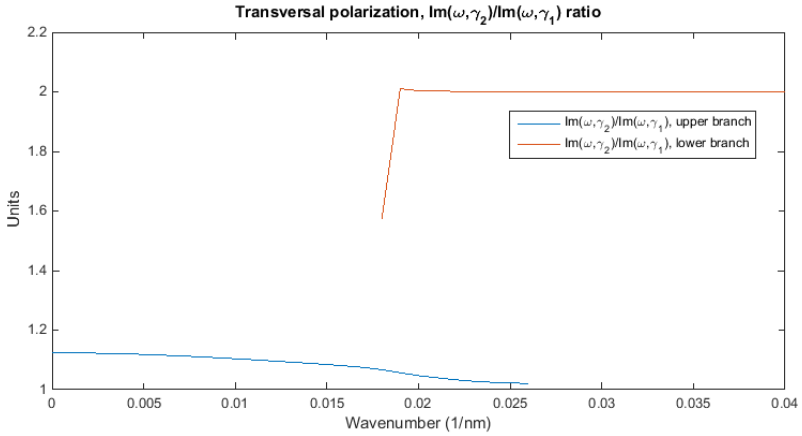

Figure 4.19: $\mathrm{Im}(\omega, \gamma_2)/\mathrm{Im}(\omega, \gamma_1)$ ratio plot for an infinite chain, real and imaginary part, for both $\gamma_1 = 0.0835$ (PHz) and $\gamma_2 = 0.167$ (PHz), transversal polarization.

The ratio for the upper branch is decreasing slightly, which includes that radiative losses decrease as the modes approximate to light line. The ratio for the lower branch gives us a nearly perfect line at 2, which indicates that the damping factor γ quantifies losses very well for these modes.

Finally, the match of the results from the dispersion relations and simulations of the chain are shown in figure 4.20. Since our plasmons travel slower than light, they are described by the lower branch of the dispersion relation.

Figure 4.20 shows that the match is very good for γ_1, while it is not very good for decays computed for γ_2. This is the same behaviour as presented in 4.17. Therefore, our chain yields

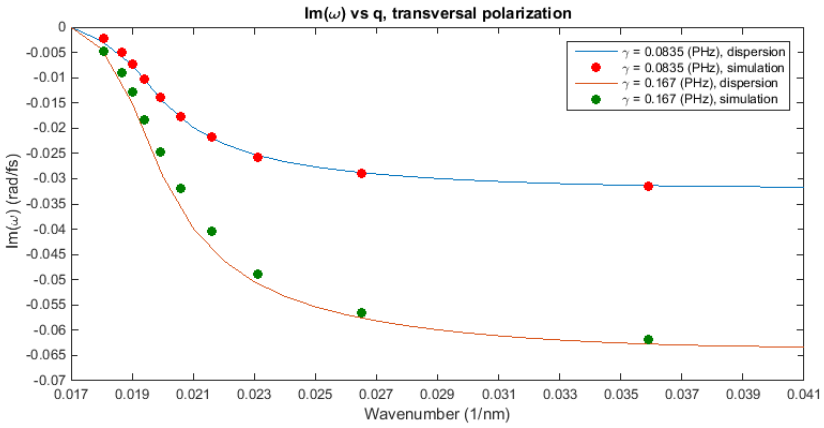

Figure 4.20: Match of the imaginary parts of the frequency obtained from the simulation of the chain's response to the dispersion relations, for $\gamma_1 = 0.0835$ (PHz) and $\gamma_2 = 0.167$ (PHz), transversal polarization.

modes closer to those that belong to an infinite chain in the regime of smaller losses, while the accuracy is lost for higher γ.

4.3.2 Group velocities

4.3.2.1 Longitudinal polarization

The definition of group velocity has been defined in equations 2.41 and 2.42. In order to get this magnitude we have derived the real part of the dispersion relation for longitudinal modes (figure 4.15, left), because group velocity is a real quantity. Note that these calculations include the assumption of an infinite chain. Our interest lies on the response of the chain for different γ, so the initial point of this subsection will be to plot the group velocities for both factors.

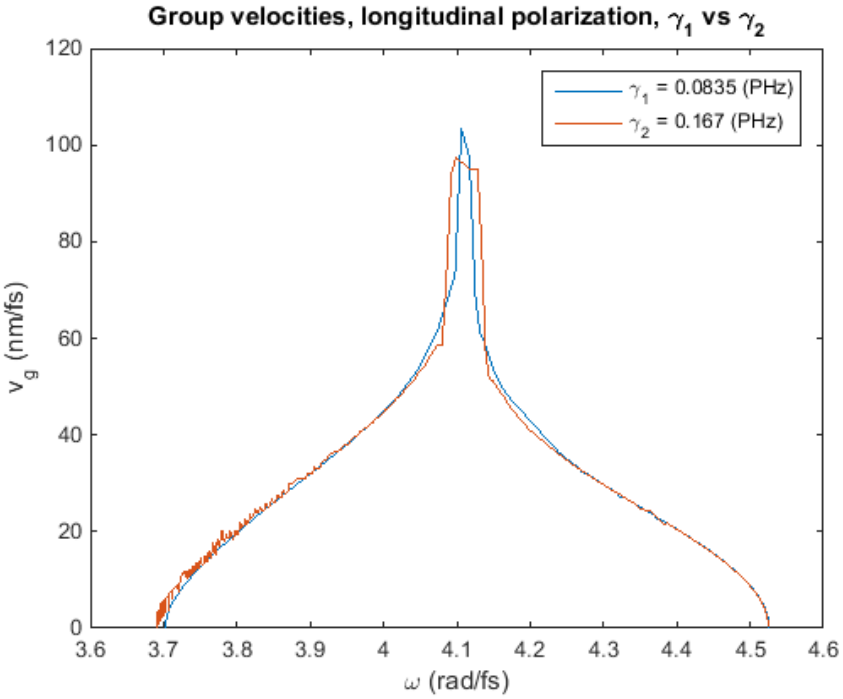

Figure 4.21: Group velocities of infinite chain for $\gamma_1 = 0.0835$ (PHz) and $\gamma_2 = 0.167$ (PHz), longitudinal polarization.

In figure 4.21 we see that both plots are similar in general, except for the values in the central peak. Therefore, together with figure 4.15, it can be said that losses do not influence the real part of the dispersion relation of the infinite chain. We look now to the match of group velocities for an infinite chain and a finite, though long enough in the nanoscale, chain of 4000 nanoparticles and length L $\approx 0.3\mu$m. We will include calculations shown in figure 4.7, and plot them for the corresponding damping factors. Note that for frequencies where diverse modes have been observed (curved plots in figure 4.7) we have split the line in shorter straight lines and calculate their slope, so that an approximate velocity for each mode is given. These velocities are plotted for the same frequency ω, and the value of the linear fit is given as an average propagation velocity of the mode. We think that its use is justified as it takes into account how far each mode propagates, taking it as a weight when calculating the fitted velocity. The match is shown in figure 4.22.

The plot in 4.22 shows that the match is very good right after the central peak of the plot. Near this peak, which is located around the point at which the light line crosses the dispersion relation, results are more ambiguous: the peak of the group velocity plot is very sharp at around $\omega = 4.1$, decreasing fast to both sides, while calculations from the chain show that at $\omega = 4.0$ – 4.1 we still have some plasmons propagating at a similar speed to that at the peak. The velocities of the different modes seen at fixed frequencies also show that the speed variation is very broad, where points are located below and considerably above the line, nearly at the velocity of light in the medium. However, we still see propagating, guided plasmons in the central region, so two possible explanations arise for the mismatch: either the plasmons in the vicinity of light line do not propagate with the group velocity, or different modes are excited in the chain for the defined

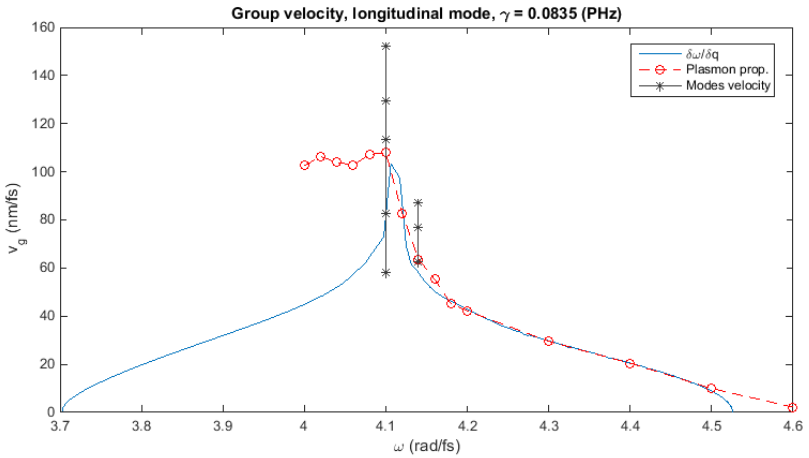

Figure 4.22: Group velocities of infinite chain compared with the velocities calculated from plasmon propagation in a finite chain of L $\approx 0.3\mu$m, for $\gamma_1 = 0.0835$ (PHz), longitudinal polarization. Other velocities are shown for frequencies where various modes have been observed (figure 4.7). A linear fit value is plotted for those cases as propagation velocity.

central frequencies, due to the $\Delta\omega$ term in the Gaussian. Further analysis will be required in order to confirm this hypothesis.

The overall trend is the same for γ_2 in figure 4.23. The matches for velocities in the region right from the peak are good again, and for frequencies where more than one mode were excited results are close. Nevertheless, the mismatch is even bigger in the central region, close to light line. As a result, we may argue that the increase of losses also enhance the mismatch between the response of the finite and infinite chain, as it has been seen in figures 4.17 and 4.20.

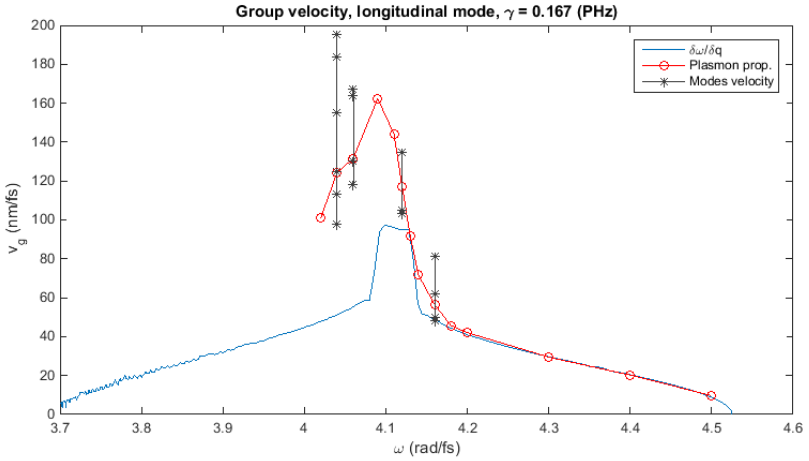

Figure 4.23: Group velocities of infinite chain compared with the velocities calculated from plasmon propagation in a finite chain of L $\approx 0.3\mu$m, for $\gamma_1 = 0.167$ (PHz), longitudinal polarization. Other velocities are shown for frequencies where various modes have been observed (figure 4.7). A linear fit value is plotted for those cases as propagation velocity.

4.3.2.2 Transversal polarization

We will do the same calculations for the transversal polarization. We start by plotting the group velocities for γ_1, γ_2 in an infinite chain in figure 4.24.

In these plots we see that the group velocity curve for smaller losses is more pronounced, while

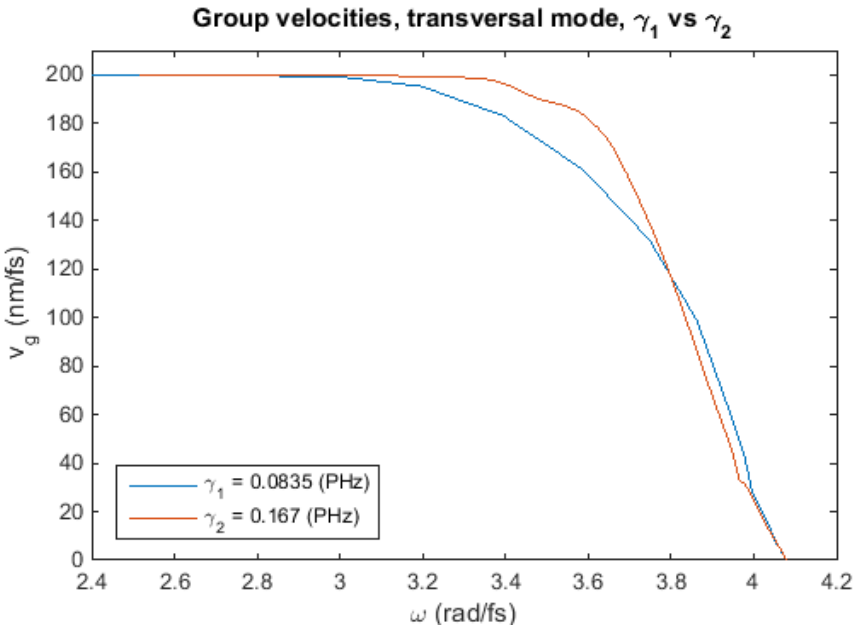

Figure 4.24: Group velocities of infinite chain for $\gamma_1 = 0.0835$ (PHz) and $\gamma_2 = 0.167$ (PHz), transversal polarization.

the plot of γ_2 starts decreasing later, until eventually both of them show the same trend. Figure 4.24 also shows that there are more transversal modes that travel at the speed of light in the medium for higher losses. We now look at the comparison between the results of the infinite chain and the finite chain for smaller damping factor γ_1 in figure 4.25.

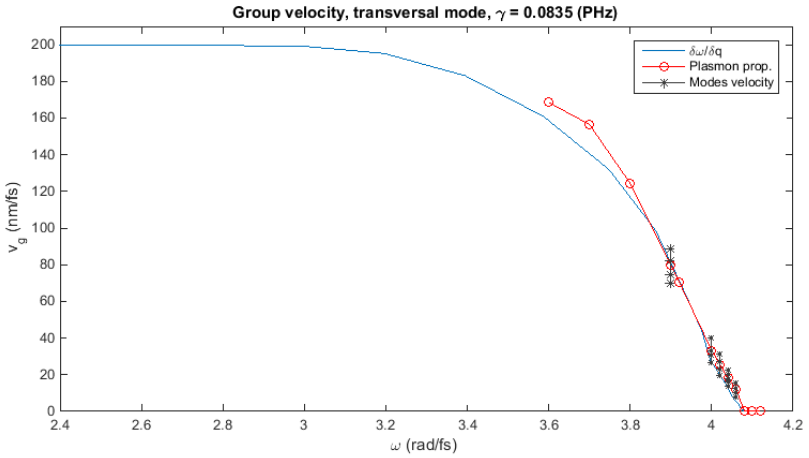

Figure 4.25: Group velocities of infinite chain compared with the velocities calculated from plasmon propagation in a finite chain of L $\approx 0.3\mu$m, for $\gamma_1 = 0.0835$ (PHz), transversal polarization. Other velocities are shown for frequencies where various modes have been observed (figure 4.13). A linear fit value is plotted for those cases as propagation velocity.

This figure shows that overall match is quite good, especially for higher frequencies. Besides, the velocities of other modes coming from 4.13 do not vary much from the dispersion relation. Finally, a similar figure is shown for γ_2 in figure 4.26.

For higher losses the match is worse, as we have already seen in previous figures in this section (4.23 for example). Some of the extra modes excited for one frequency match the frequency well, but they are isolated cases. In general, we can confirm that higher losses produce bigger mismatch

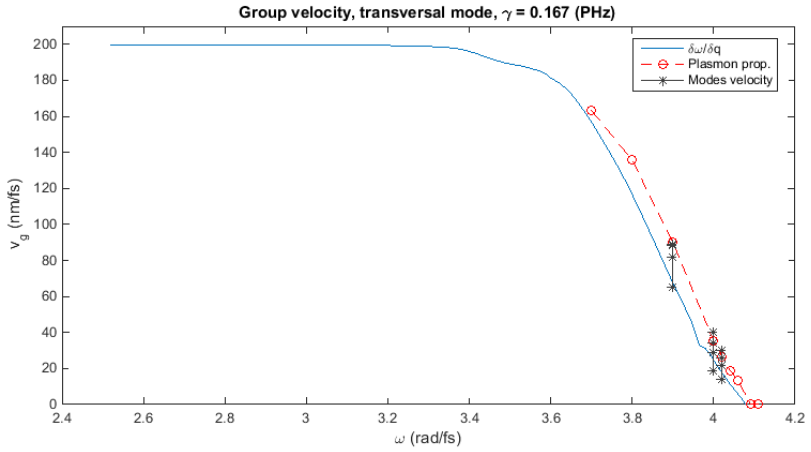

Figure 4.26: Group velocities of infinite chain compared with the velocities calculated from plasmon propagation in a finite chain of L $\approx 0.3\mu$m, for $\gamma_2 = 0.167$ (PHz), transversal polarization. Other velocities are shown for frequencies where various modes have been observed (figure 4.13). A linear fit value is plotted for those cases as propagation velocity.

between the responses of a finite and infinite chain.

4.4 Energy transport of the chain

The previous section, in particular the analysis of group velocities, have shown that little can be said about plasmonic modes which are close to the light line. We have suggested that at these frequencies plasmons might have different propagation velocities than the group velocity. An alternative was the energy transport velocity, which is calculated from the Poynting vector and the energy density of the plasmon. Comparing this to the previous obtained results can give us more insight in the physics of the problem.

We start by looking at the propagation of the Poynting vector. As it has been said in section 2.5, the Poynting vector describes the energy flux density along a particular direction. Since our chain lies in the previously defined $\hat{x}$-direction, we will look at the $\hat{x}$-component of the Poynting vector defined in Cartesian coordinates to see the energy transport in this direction. We set a plane between particles 800 and 801, defined by coordinates y and z, and we will look at the values calculated in different points in the plane. This plane has dimensions 400×400 (nm) and it is centered at point (0,0). Due to retardation effects and signal decay, only the nearest 200 particles near the plane contribute to the generation of electromagnetic fields in the plane.

4.4.1 Longitudinal polarization

In the longitudinal polarization, the dipole moments are polarized in $\hat{x}$-direction. Therefore, we do not expect to see any energy flux in the $\hat{x}$-axis passing through the center of the plane (0,0), as this is the line where the dipole moments lie. On the other hand, we need to make sure that the plasmon passes through our plane: for this purpose, a central frequency of $\omega_0 = 4.18$ (rad/fs) and the damping factor $\gamma_1 = 0.0835$ (PHz) have been chosen as initial parameters, as from figure 4.3 we expect to see a plasmon there. We will now show the magnitude of the $\hat{x}$-component of the Poynting vector and the electromagnetic energy density as a function of time, evaluated in a point of the plane close to the center.

From figures 4.27 and 4.28 we can see that there are two peaks that happen at similar times: the first and highest peak corresponds to the main pulse propagating in the chain at the speed of light in the medium, while the second peak represents the plasmon. The next step is to show both quantities in the plain at both maxima.

The planar distribution of figure 4.29 looks similar in both cases; nevertheless, if we look at the scales, the values for the plasmon are smaller, as we expect to see from figures 4.5 and 4.6. Departing from this results, we calculate the energy transport velocity: we have done so by integrating numerically the Poynting vector and EM energy density over time. Nevertheless, we have not obtained any coherent result from here which would match the propagation speed of plasmons. As an alternative, the integrals of the Poynting vector and the electromagnetic energy density have been calculated over the plane, but no improvement has been achieved. Consequently, we will not be able to give more insight on the mismatch of plasmon velocities and group velocities, as our alternative method has not been successful.

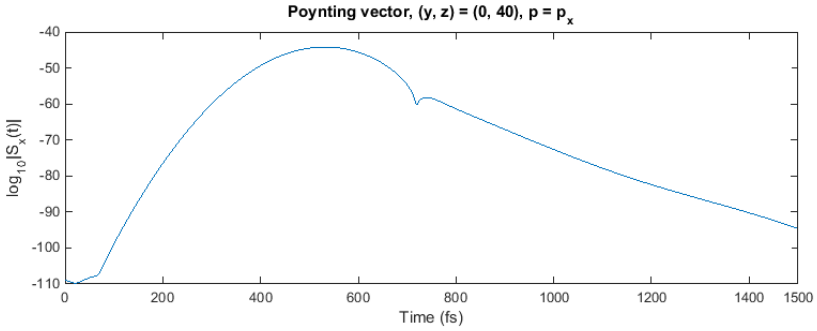

Figure 4.27: Logarithm of the amplitude of the $\hat{x}$-component of the Poynting vector for a longitudinal mode as a function of time in a chain of 4000 particles. The evolution of the vector in a point near the center of the plane is shown. Note that $\omega_0 = 4.18$ (rad/fs) and $\gamma = 0.0835$ (PHz).

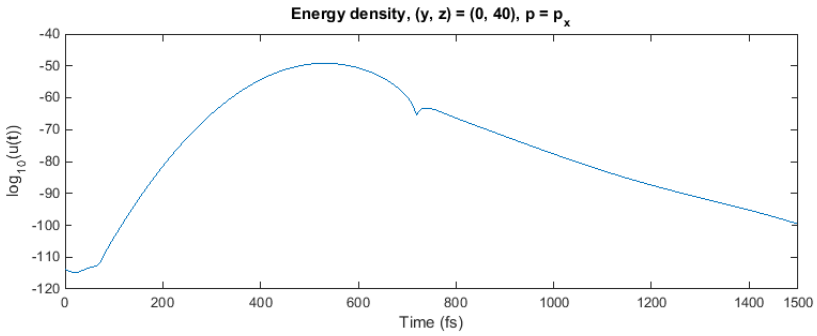

Figure 4.28: Logarithm of the energy density for a longitudinal mode as a function of time in a chain of 4000 particles. The evolution of the magnitude in a point near the center of the plane is shown. Note that $\omega_0 = 4.18$ (rad/fs) and $\gamma = 0.0835$ (PHz).

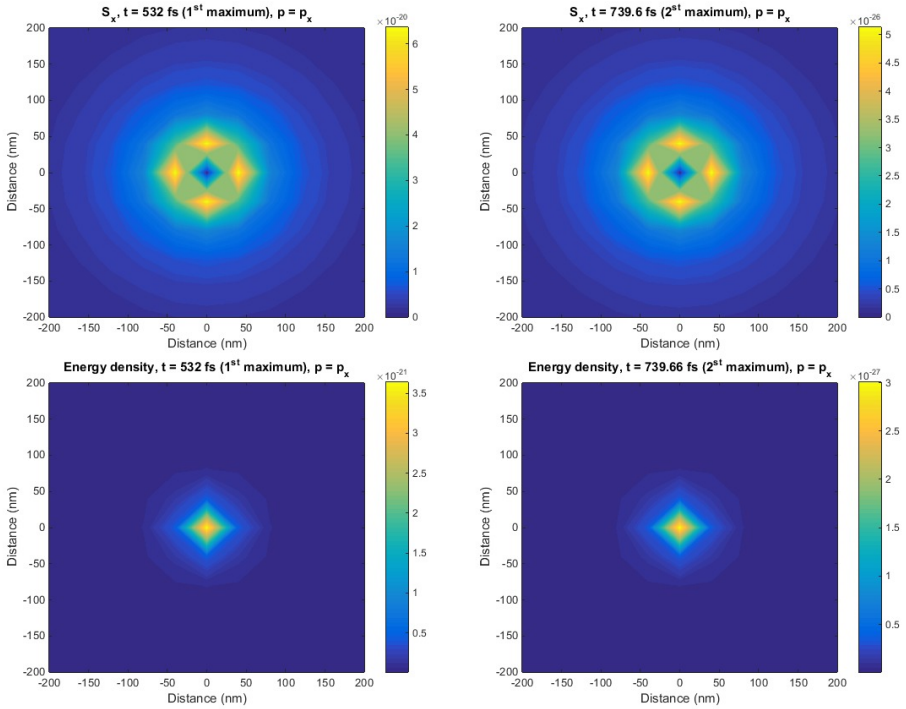

Figure 4.29: Amplitude of the $\hat{x}$-component Poynting vector and energy density represented in a plane perpendicular to the chain of 4000 particles, placed between particles 800 and 801, for longitudinal polarization. $\omega_0 = 4.18$ (rad/fs) and $\gamma = 0.0835$ (PHz).

4.4.2 Transversal polarization

The analogous of the previous subsection for transversal modes is developed here. Since all dipoles are polarized perpendicular to the chain, the Poynting vector and the electromagnetic energy density can safely be evaluated at the center of the plane. The method is the same as we have used for the longitudinal case, so we will just present the results now. The plane remains between particles 800 and 801; the parameters chosen for the excitation of plasmons are $\omega_0 = 3.9$ (rad/fs) and the damping factor $\gamma_1 = 0.0835$ (PHz), which stays invariant with respect to the energy calculations of the longitudinal case. Figure 4.10 shows that for the defined parameters the plasmon reaches our plane set between particles 800 and 801.

In general, figures 4.27 and 4.28 for longitudinal polarization and figures 4.30 and 4.31 show both the forerunner and the plasmon peaks. Besides, plane contours (figures 4.29 and 4.32 show nicely the different patterns of the propagating fields, which might be interesting and useful for further research. Nevertheless, our aim of calculating energy velocities has not been fulfilled due to failures in the developed methods.

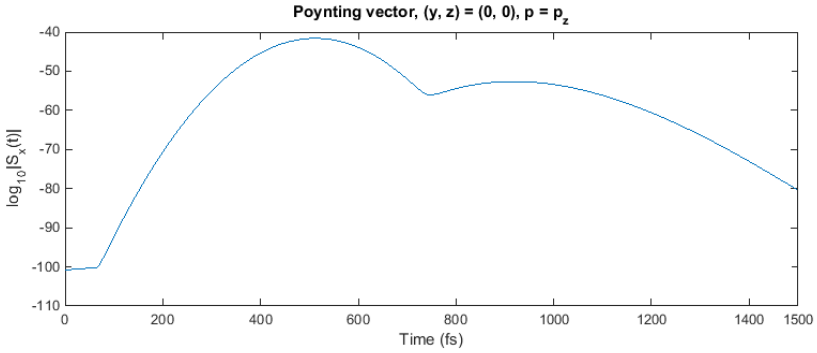

Figure 4.30: Logarithm of the amplitude of the $\hat{x}$-component of the Poynting vector for a transversal mode as a function of time in a chain of 4000 particles. The evolution of the vector in a point near the center of the plane is shown. Note that $\omega_0 = 3.9$ (rad/fs) and $\gamma = 0.0835$ (PHz).

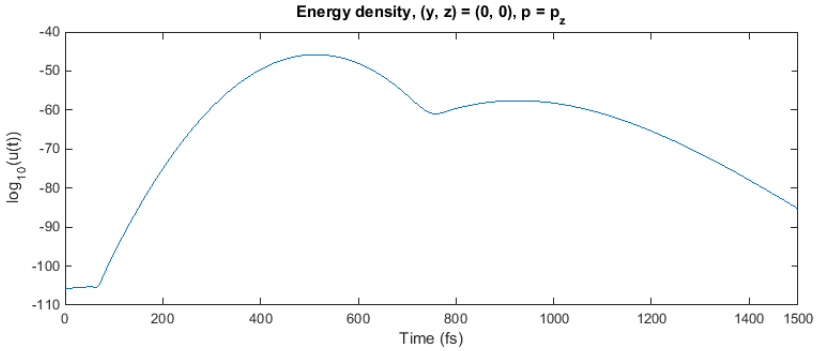

Figure 4.31: Logarithm of the energy density for a longitudinal mode as a function of time in a chain of 4000 particles. The evolution of the magnitude in a point near the center of the plane is shown. Note that $\gamma = 0.0835$ (PHz).

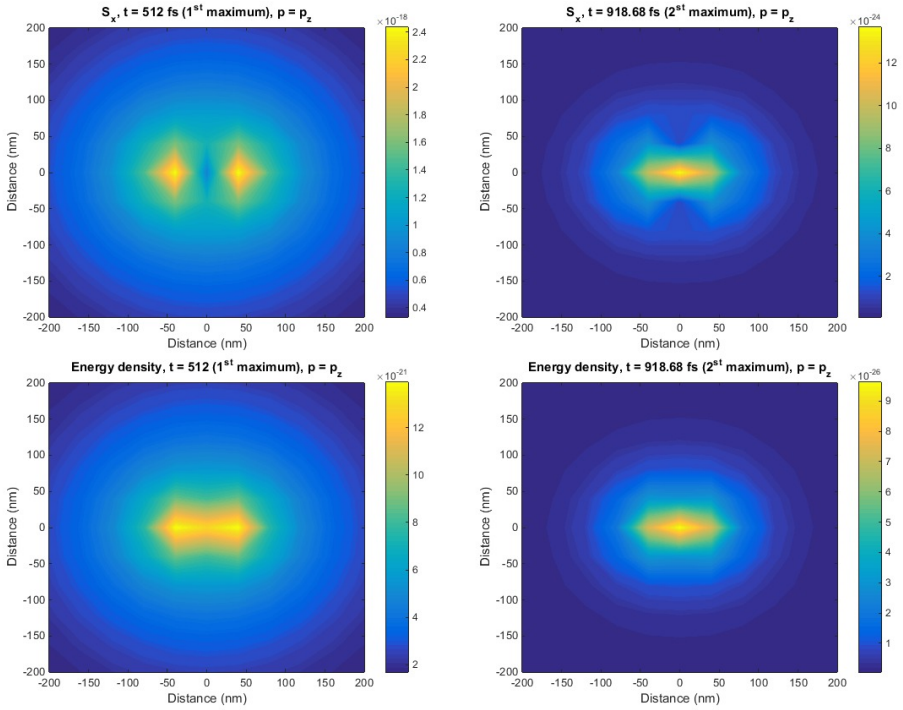

Figure 4.32: Amplitude of the x-component Poynting vector and energy density represented in a plane perpendicular to the chain of 4000 particles, placed between particles 800 and 801, for transversal polarization. $\omega_0 = 3.9$ (rad/fs) and $\gamma = 0.0835$ (PHz).

4.4.3 New insight in the energy velocity problem

In order to try to compensate the lack of results regarding plasmon velocity of this section, we will introduce a new method to calculate this quantity of interest. We argue that the origin of our difficulties lies on the fact that the plasmon consists of the sumation of different oscillating terms: it is a superposition of different modes. Due to its propagation in dispersive media, the dispersion relation for these modes is a complicated expression involving wavevector k and its frequency $\omega(k)$, as it has been shown in section 2.4 of this work. Figure 2.1 shows the shape of this relation. Therefore, we introduce a new perspective for calculating propagation velocities by considering the superposition of various modes, i.e. a wave packet.

We consider the electric field of the plasmon as a superposition of plane waves with unknown dispersion relation $\omega(k)$. The vector is in $\hat{z}$-direction. The wave packet is given by the following equation:

$$\vec{E}(x,t) = \frac{\hat{z}}{2\pi}\int_{-\infty}^{\infty} e^{-\frac{(k-k_0)^2}{4}} e^{ikx - i\omega(k)t} dk \tag{4.1}$$

This equation already takes into account the Gaussian amplitude of the wave packet, which originates from the different coefficients of the superposing waves. Since the dispersion relation $\omega = \omega(k)$ is known, we claim that this method can help us obtain the exact velocities in the dispersive medium, which in our system is a kind of effective media consisted of silver (dispersive) and the glass between particles (non-dispersive).

We will now show the validity of this suggestion by assuming a linear dispersion relation: $\omega = vk$. Solving equation 4.33 gives that the electric field in the $\hat{z}$ direction is:

$$\vec{E}(x,t) = e^{(x-vt)^2 + ik_0(x-vt)}\hat{z} \tag{4.2}$$

Inserting 4.2 in Faraday's equation (eq. 2.17), the magnetic field is:

$$\vec{H}(x,t) = -\frac{1}{v\mu_0\mu_m} e^{(x-vt)^2 + ik_0(x-vt)}\hat{j} = -\frac{1}{v\mu_0\mu_m}|E|\hat{j} \tag{4.3}$$

where $|E|$ is the magnitude of the electric vector. Since these are plane waves, we can use equations 2.48, 2.49 and 2.51 in order to obtain the energy transport velocity. We remind that $v = c/n = 1/\sqrt{\epsilon_0\epsilon_m\mu_0\mu_m}$. We finally develope the following equation:

$$\begin{aligned} v_E = & \frac{\left\langle \vec{S} \right\rangle}{\langle W \rangle} = \frac{\frac{1}{2}Re[\vec{E}\times\vec{H}^*]}{\frac{1}{4}(\epsilon_0\epsilon_m|E|^2 + \mu_0\mu_m|H|^2)} = \\ & = \frac{2|E|\frac{1}{v\mu_0\mu_m}|E|}{\epsilon_0\epsilon_m|E|^2 + \frac{\mu_0\mu_m}{v^2\mu_0^2\mu_m^2}|E|^2}\hat{i} = \frac{\frac{2}{v\mu_0\mu_m}}{\epsilon_0\epsilon_m + \frac{\epsilon_0\epsilon_m\mu_0^2\mu_m^2}{\mu_0^2\mu_m^2}}\hat{i} = \\ & = \frac{\frac{2}{v\mu_0\mu_m}}{\epsilon_0\epsilon_m + \epsilon_0\epsilon_m}\hat{i} = \frac{1}{v\epsilon_0\epsilon_m\mu_0\mu_m}\hat{i} = \frac{v^2}{v}\hat{i} = v\hat{i} \end{aligned} \tag{4.4}$$

Therefore, we show that the energy transport velocity can be calculated using this analysis, since the result agrees with what we expected: energy transport velocity v_E is equal to the group velocity v, which at the same time equals phase velocity.

Finally, the propagation of this wave packet in space and time is shown in figure 4.33, where $k_0 = 0.023$ (1/nm). The propagation with constant velocity is clear there.

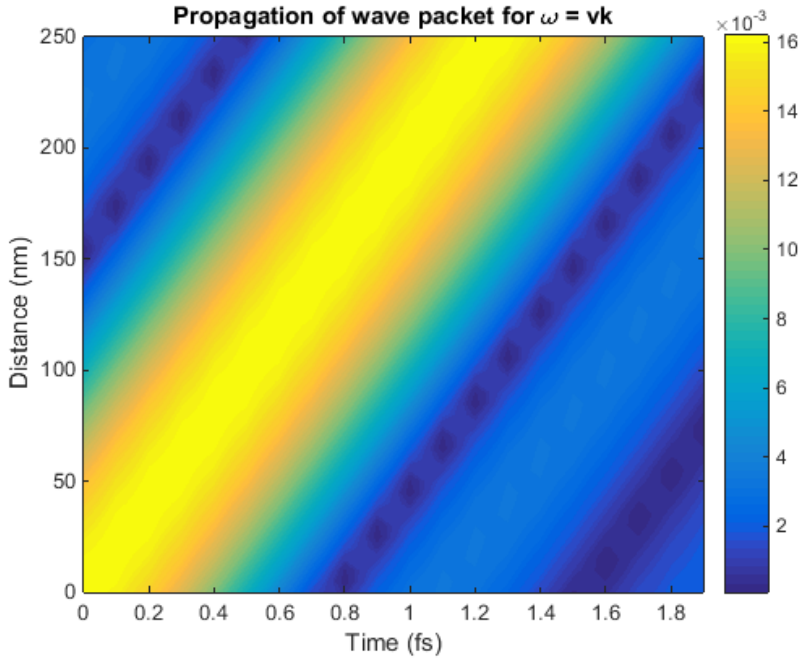

Figure 4.33: Propagation of wave packet with linear dispersion relation $\omega = vk$, where v is the group velocity and k the wave vector.

Chapter 5

Conclusions

In this work a chain of 4000 silver spherical nanoparticles embedded in glass has been modeled, and a propagating wave packet along the system has been simulated. The response of the chain to a propagating signal has been compared to the wave-guiding properties of an infinite chain, derived from the dispersion relation. The first particle of the chain has been excited with a electric field pulse of Gaussian shape: the direction of the electric field vector was either parallel (longitudinal polarization) or perpendicular (transversal polarization) to the axis of the chain. The propagation of the electromagnetic fields along the chain and the consequent excitation of oscillating electric dipole moments in each nanoparticle have been calculated using the dyadic Green's functions. In order to determine the properties of the silver particles, such as polarizability and dielectric permittivity, an experimentally fitted Drude model has been taken into account. This model includes Ohmic damping factor γ, which determines the losses of the system. A particular interest have been shown in the influence of losses in the response of the chain; as a result, calculations have been carried on for damping factors γ_1 and γ_2, being the value of the first half of that of the second term.

The excitation of the first particle by a Gaussian pulse has yielded two propagating modes along the chain. The first mode is the $forerunner$, which travels along the chain with the speed of light in the medium. The second mode is the *surface plasmon*, which decays faster, thus has a shorter lifetime. The influence and effect of losses in the propagation of plasmonic modes has been analysed for two damping factors. In general, lifetime and propagation length decrease due to an increase of the damping term. Conclusions are presented for different polarizations of the plasmon: longitudinal and transversal.

The increase of losses in the dispersion relation of an infinite chain for longitudinally polarized modes have shown no variation for the real part of the modes and the group velocities. Imaginary parts of the modes have increased in magnitude, as expected. The comparison of the results from the finite chain show a good match for the imaginary parts of the modes in the region below the light line, but the fit for smaller losses suggested a better match. Near the intersection of the modes with light dispersion results were worse for both cases, as it was expected due to the radiative losses that arise in that region. Group velocities calculated from dispersion relation displayed a very good match between them for both γ_1 and γ_2, with a slight difference in the light-crossing region. The comparison with the results coming from the finite chain have shown more disagreements. The match for group velocities of the dispersion relation and plasmon propagation velocities are very good below the light line for both damping factors. Nevertheless, in the vicinity of the light line, there is a big mismatch, the latter being bigger for larger losses. Therefore, it is suggested that the plasmonic modes excited nearby the light-plasmon dispersion intersection in the chain are not the same as the modes excited in the infinite chain. A support for this hypothesis comes from the observation of different longitudinal modes at a given central frequency in the range $\omega_0 = 4.0$ - 4.2 (rad/fs), which give raise to velocities within a broad band around the group velocities. It is noted that at this frequency range the chain modes are close to the dispersion of light. Another option is that the plasmons travel with energy velocity transport.

Transversal modes of the finite chain below the light line are in good agreement with dispersion relations of the infinite chain. The real part of dispersion relation remains invariant under the increase of losses, so excitation of the same modes is preserved. The expected increase in the absolute value of the imaginary part is well followed by the response of the finite chain; however, the results for bigger damping factor confirm that the match between the modes of the finite and infinite chain are worse for higher losses.

Group velocities calculated from dispersion relation have shown some differences for the two γ factors. Simulations in the finite chain show the same trend as the calculated group velocity, results from smaller losses being in better agreement with the group velocities. Other excited modes for single central frequencies disperse much less around the given group velocities than for the longitudinal case. This shows that in the transversal case the velocity of plasmons agrees well with group velocities of modes in an infinite chain for small losses. Besides, the additional modes have been observed for frequency range $\omega_0 = 3.9$ - 4.1 (rad/fs), which corresponds to the region where the dispersion relation of plasmon modes under the light line separates from the light line. These results, along with the fact that the frequency range of various excited modes in the longitudinal polarization is also close to the intersection with light, suggest that various modes can be excited at this regime.

Finally, the basis for the calculation of energy transport velocity was set in order to perform such calculations. The excited modes in the chain for a single central frequency, namely the forerunner and the plasmon, show up themselves in the plots of the electromagnetic fields as a function of time. Results of the plane show nicely the patterns for propagation of electromagnetic fields along the chain. Interesting tools have been developed to treat the plasmon propagation from the energy transport point of view; unfortunately, methods designed for calculating the energy transport velocity have not been productive. It is suspected that the superposition of various modes with frequencies to be determined from dispersion relations have been the origin of this failure. Due to that, a wave packet solution has been introduced. Its validity have been shown for linear dispersion relations, where no dissipation along the propagation is expected.

This chapter will be concluded with some suggestions for future research. Disagreement of modes in finite and infinite chain for the longitudinal polarization arises close to the intersection point between the dispersion relation of light and the chain, showing plasmons propagating at different velocities. Furthermore, it has been seen that the width of the Gaussian in the frequency domain generates other modes for central frequencies around the light line. It can be helpful to check the veracity and the origin of this, and in the case of a positive response, try to calculate these other modes, which might be in accordance with the unmatched plasmonic velocities of the chain. On the other hand, fixing the problems of the calculations regarding energy transport velocity is another strong candidate for future work, since it promises good insight into the physics of the problem. The application of the wave packet analysis for the dispersion relation of the chain seems to be a promising tool to obtain good results for propagation velocity calculations.

Chapter 6

Acknowledgements

In the first place I would like to thank Jasper Compaijen for his guidance, wise comments and valuable and helpful advises during the realization of this project. Many thanks as well due to his dedication and patience. Furthermore, I would also like to thank Prof. dr. Jasper Knoester for his supervision and suggestions. Besides, I would like to remember all the people who, through direct participation in the project or either motivating and cheering me, contributed so much throughout this research. Finally, I want to express my gratitude to Rijksunivesiteit Groningen (RUG) for providing an exchange student with the opportunity and all the facilities to conduct this work.

To conclude with, thanks to Dr. Jon Urrestilla Urizabal from Euskal Herriko Unibertsitatea (EHU) for his assistance during the last steps of the conclusion of this work.

Chapter 7

Bibliography

[1] W. L. Barnes, A. Dereux, and T. W. Ebbesen. Surface plasmon subwavelength optics. *Nature* **424**, 824-830 (2003).
[2] J. R. Sambles, G. W. Bradbery, and Fuzi Yang. *Contemporary Physics* **32**, 173-183 (1991).
[3] S. A. Maier. *Plasmonics: Fundamentals and Applications.* Springer, New York, 2007.
[4] R. Gordon, A. G. Brolo, D. Sinton, and K. L. Kavanagh. Resonant optical transmission through hole-arrays in metal films: physics and applications. *Laser & Photon. Rev.* **4**, 311-335 (2010).
[5] S. Anantha Ramakrishna. Physics of negative index materials. *Rep. Prog. Phys.* 68, 449–521 (2005).
[6] P. J. Compaijen, V. A. Malyshev, and J. Knoester. Engineering plasmon dispersion relations: hybrid nanoparticle chain – substrate plasmon polaritons. *Opt. Express* **23**, 2280-92 (2015).
[7] M. Meier and A. Wokaun. Enhanced fields on large metal particles: dynamic depolarization. *Optics Letters* **8**, 581 (1993).
[8] L. Novotny and B. Hecht. *Principles of Nano-Optics.* Cambridge University Press, Cambridge, UK, 2006.
[9] A. F. Koenderink, R. De Waele, J. C. Prangsma, and A. Polman. Experimental evidence for large dynamic effects on the plasmon dispersion of subwavelength metal nanoparticle waveguides. *Physical Review B* **76**, 201403 (2007).
[10] L. A. Sweatlock, S. A. Maier, H. A. Atwater, J. J. Pennikhof, and A. Polman. Highly confined electromagnetic fields in arrays of strongly coupled Ag nanoparticles. *Physical Review B* **71**, 235408 (2005).
[11] J. D. Jackson. *Classical Electrodynamics.* John Wiley & Sons, Inc., third edition, 1999.
[12] W. H. Weber and G. W. Ford. Propagation of optical excitations by dipolar interactions in metal nanoparticle chains. *Physical Review B* **70**, 125429 (2004).
[13] A. F. Koenderik and A. Polman. Complex response and polariton-like dispersion splitting in periodic metal nanoparticle chains. *Physical Review B* **74**, 033402 (2006).
[14] F. W. J. Olver, D. W. Lozier, R. F. Boisvert, and C. W. Clark. *NIST Handbook of Mathematical Functions.* Cambridge University Press, New York, 2010.
[15] A. Jonquière. *Bulletin de la Société Mathématique de France 17*, 142-152 (1889).
[16] L, Ahlfors. *Complex Analysis.* McGraw-Hill, Inc., third edition, 1979.
[17] L. Brillouin. *Wave Propagation and Group Velocity.* Academic Press, New York, 1960.
[18] P. de Vries, D. V. van Coevorden, and A. Lagendijk. *Rev. Mod. Phys.* **70**, 447 (1998).
[19] R. Ruppin. Electromagnetic energy density in a dispersive and absorptive material. *Physics Letters A* **299**, 309–312 (2002).
[20] L.D. Landau, E.M. Lifshitz. *Electrodynamics of Continuous Media*, Pergamon, Oxford, 1960.
[21] Fast Fourier Transform. *http://nl.mathworks.com/help/matlab/ref/fft.html.*